DANMARKS OG GRØNLANDS GEOLOGISKE UNDERSØGELSE RAPPORT 2005/74

Site description, geological settings and core and soil sampling at the Kluczewo Airport, Poland

Deliverable report of D2 and D3 to EU in relation to contract no. SSPI-CT-2003-004017

Klint, K. E., Kasela, T., Nilsson, B. & Haessler, F.

GEOLOGICAL SURVEY OF DENMARK AND GREENLAND
MINISTRY OF THE ENVIRONMENT

G E U S

DANMARKS OG GRØNLANDS GEOLOGISKE UNDERSØGELSE RAPPORT 2005/74

Site description, geological settings and core and soil sampling at the Kluczewo Airport, Poland

Deliverable report of D2 and D3 to EU in relation to contract no. SSPI-CT-2003-004017 STRESOIL

Klint, K. E., Kasela, T., Nilsson, B. & Haessler, F.

GEOLOGICAL SURVEY OF DENMARK AND GREENLAND
MINISTRY OF THE ENVIRONMENT

GEUS

ABOUT THIS DOCUMENT

This report is a joint report of the deliverables D2 and D3 of the Stresoil Project.

Title	Deliverable D2 and D3. Site description, geological settings and core and soil sampling at the Kluczewo Airport, Poland
Purpose	Deliverable report of D2 and D3 to EU in relation to Contract No. SSPI-CT-2003-004017
Filename	Stresoil-Deliverable report D2-D3.doc
Authors	Knud Erik Klint, Tomasz Kasela, Bertel Nilsson and Frank Haessler
Document history	Progress report
Current version	4
Changes to previous version	Not applicable
Date	15/11/05
Status	final
Target readership	European Commission and Steering Committee
General readership	Project members
Correct reference	Klint K.E., Kasela T., Nilsson B. and Haessler F., 2005: Site description, geological settings and core and soil sampling at the Kluczewo Airport, Poland. Deliverable report of D2 and D3. GEUS report no. 74. pp 0-34.

TABLE of Content

1. Introduction

This report was written as part of the 1st Annual report for the EU-project STRESOIL.
Work Package 1. The report contains a description of the fieldwork accomplished so far, a detailed geological model and a conceptual macropore model representative for the site. The distribution of contamination is described as well as the sampling of sediment samples for laboratory experiments.

The report cover the documentation for the following deliverables:

- D2: Collection of soil samples, groundwater samples and intact samples of fractures and contaminated water samples.
- D3 Geological/hydrogeological /geotechnical model.

The report was prepared according to the following milestones:

- M1. Report describing the preliminary 3D Geological model of the site
- M3. Report on preliminary Hydrogeological model
- M4. Report on establishment of 3-4 deep pits on the site

2. Goals and Scopes

The goal of WP1 is: Site characterisation and mapping of the NAPL distribution on the site. This includes construction of a general and local geological/hydrogeological model; mapping of the distribution and fate of NAPL over the site; and finally development of fracture network / matrix porosity models.
The following tasks area specified in WP1:

TASK 1-1 Multiscale hydrogeological characterisation of the site

- Collection and organisation of existing data and information about the site.
- Construction of a geological model, and description of the geological history of the area.

TASK 1-2 Core and soil sampling

TASK 1-3 Development of a conceptual geological/fracture model of the site

- Detailed description of the tectonic history of the area and classification of the glacigene sediments.
- Classification and characterisation of the fractures into fracture systems with characteristic properties.
- Calculations of quantitative fracture properties for each fracture system, primarily spacing of the individual fracture systems.
- Collection of additional intact samples of fractured sediment for impregnation and measurement of the mechanical fracture aperture (opening diameter) on intact samples of fractured rocks.
- Construction of a conceptual macroscopic fracture network model.

TASK 1-4 Determination of the spatial distribution of NAPL over the site

TASK 1-5. Microbiological characterisation of the site

3. Site description

Historical description

The selected site is situated on the former Kluczewo airport in Poland The Kluczewo airport is situated approximately 4-5 km west of a lake Miedwie and south of the city Stargard Szczecinski in the north-western part of Poland (fig. 3.1 and 3.2).

Fig. 3.1 Location of the Kluczewo airport.

Fig. 3.2 Kluczewo airport

Germany (1927-1945) and Soviet Union (1946-1992) used the airport for primary military purposes. The former Kluczewo Airport is the second largest ground-water reservoir contaminated by fuel in Poland, and growing concern for the future water supply to the city of Stettin led to investigations of the potential hazard to contamination of Lake Miedwie.

In the period 1993-1996, the contaminated areas were investigated. The regional groundwater flow is directed towards the Lake Miedwie. The contaminated sediments consist of 3-7 meters thick clayey diamict sediments that overlie up to 10 meter of meltwater sand. The total known area of contamination was approximately 38 ha in 1993, with a volume of contaminated diamict sediments at approximately 950.000m^3 and approximately 1.450.000 m^3 of contaminated meltwater sand (in 1993). After additional geological investigation the total area of contaminated grounds was estimated to be about 50 ha (in 1996).

Earlier projects.

Actions towards remediation of the site were initiated in 1994. During the next 8 years Hydrogeotechnica carried out an extensive clean-up programme in corporation with local authorities. In the period ranging from 1994 until today a total amount of *ca* 1800m^3 free phase LNAPL (pure jet fuel), has been skimmed from the surface of the groundwater. Additional free phase LNAPL has also been removed by locals from primitive wells that are scattered throughout the area. The total amount is unknown, but it is has been reported that approximately 3 m^3 may be skimmed from such a well in one year. The skimming programme was abandoned in the fall 2004 because it is evaluated that a total removal of the remaining LNAPL is technically and economically not feasible today. A large amount of contamination is however still remaining primarily within the fine-grained glacigene deposits overlaying the sandy aquifer. The scope of the present research project is accordingly focused on combining new stimulation technologies with viable remediation technologies for reduction of contamination within these low-permeable fractured sediments.

4. Geological settings

Regional geological setting for the Kluczewo airport

The airport is located about 4 km west of Lake Miedwie, which forms the primary drinking water reservoir for the city of Stettin. The airport and the areas that have been contaminated are marked on Fig. 4.1. The test site is situated in the central part of the airport, where extensive pollution have taken place from leaking fuel tanks and pipelines.

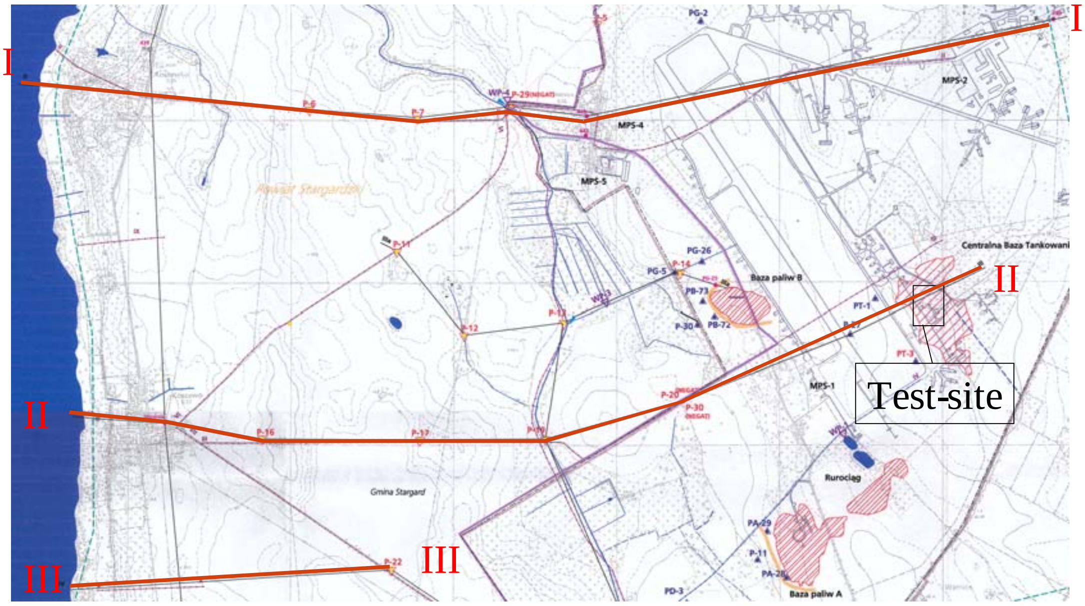

Fig. 4.1 Site map of the Kluczewo airport. The geological cross-sections I, II and III are marked on the map (See fig. 4.2) Contaminated areas are marked with red. The test site is situated in the centre of a large contaminated area close to some former fuel tanks.

The geological framework in the area is dominated with glacigene sediments of primarily Weichselian age overlaying pre-Quaternary sediments consisting of clay silt and coal-beds. On Section III (fig. 4.2) a geological section reaching from the test-site towards the Lake Miedwie. As showed on the section the area that is covered with 3-8 meters of fine-grained sediments that has been classified as clay till or lacustrine clay. The clay till has been correlated to the so-called Pomeranian ice-advance (approximately 15.000 BP) that also correlates to the Young Baltic Ice-advance in Denmark (Houmark-Nielsen and Kjaer 2003). The till is between 5 and 8 meters thick over the testsite, and the water table is generally confined approximately 4.5-5 meters below the ground surface. These fine-grained beds overlie a regional distributed occurrence of glaciofluvial sand that forms the primary aquifer in the region. The sand varies between 4 and 15 meters in thickness, with a typical thickness of 6-10 meter below the test site. The glaciofluvial sand overlays another clay-till unit that origin from a former ice-advance probably the main ice-advance (Houmark-Nielsen and Kjaer 2003) that reached far into Poland and Germany during the glacial maximum of the late Weichselian (24-21.000 BP). The till is widespread in most of the area and varies in thickness between 8-20 meters. Below this till older glacigene deposits overlay the pre-Quaternary sediments and the total thickness of the Quaternary sediments range generally between 20 and 50 meters, but exceeds 80 meters where large river valleys are eroded deep into the pre-Quaternary beds.

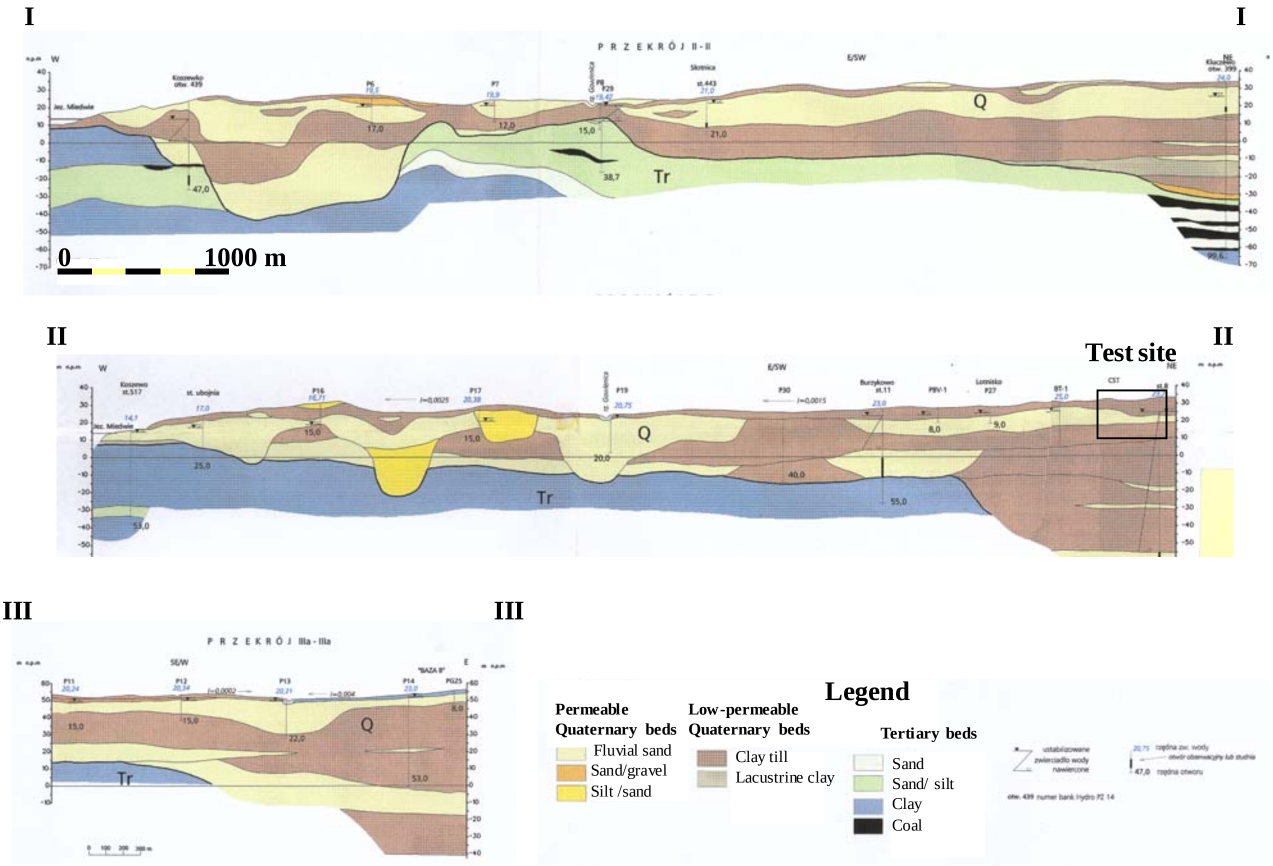

Fig. 4.2 Geological cross-sections showing the distribution of sediments within the area (based on well data and geological maps. Section II includes the test site.

Local geological model for the test area

The area was surveyed during the period Aug. 24-26. 2004.

A large part of the selected test site has been abandoned since the airport closed in 1992 and vegetation has occupied most of the area. The leaking tanks and much of the constructions have been removed and only some nearby buildings and the berms that were shielding the tanks are left above ground surface along with concrete foundations for the tanks. The long history of activity have naturally resulted in numerous installations underground (cables, pipes, tunnels, old wells, tanks) and various buried metal junk like parts of aircraft's and other machinery. The junk are primarily restricted to the upper 2 meters of the ground, but in some areas tunnels are situated deeper than 3 meters below ground surface. All these leftovers are covered by the general term "fill" in the following description. A careful survey of the site was carried out in order to classify the sediments and locate three suitable locations for the experimental cells. The general criteria was to avoid too much “fill”, but still operate in an area with a considerable amount of contamination. Originally we would also favour an area with more or less the same geological framework in order to make a good comparison between the three cells. Initially a large pit (PIT 1 fig. 4.3) were excavated down to 4,5 meter below ground surface along with 4 trenches that were excavated to approximately 2,5 meter below ground surface (Fig. 4.3).

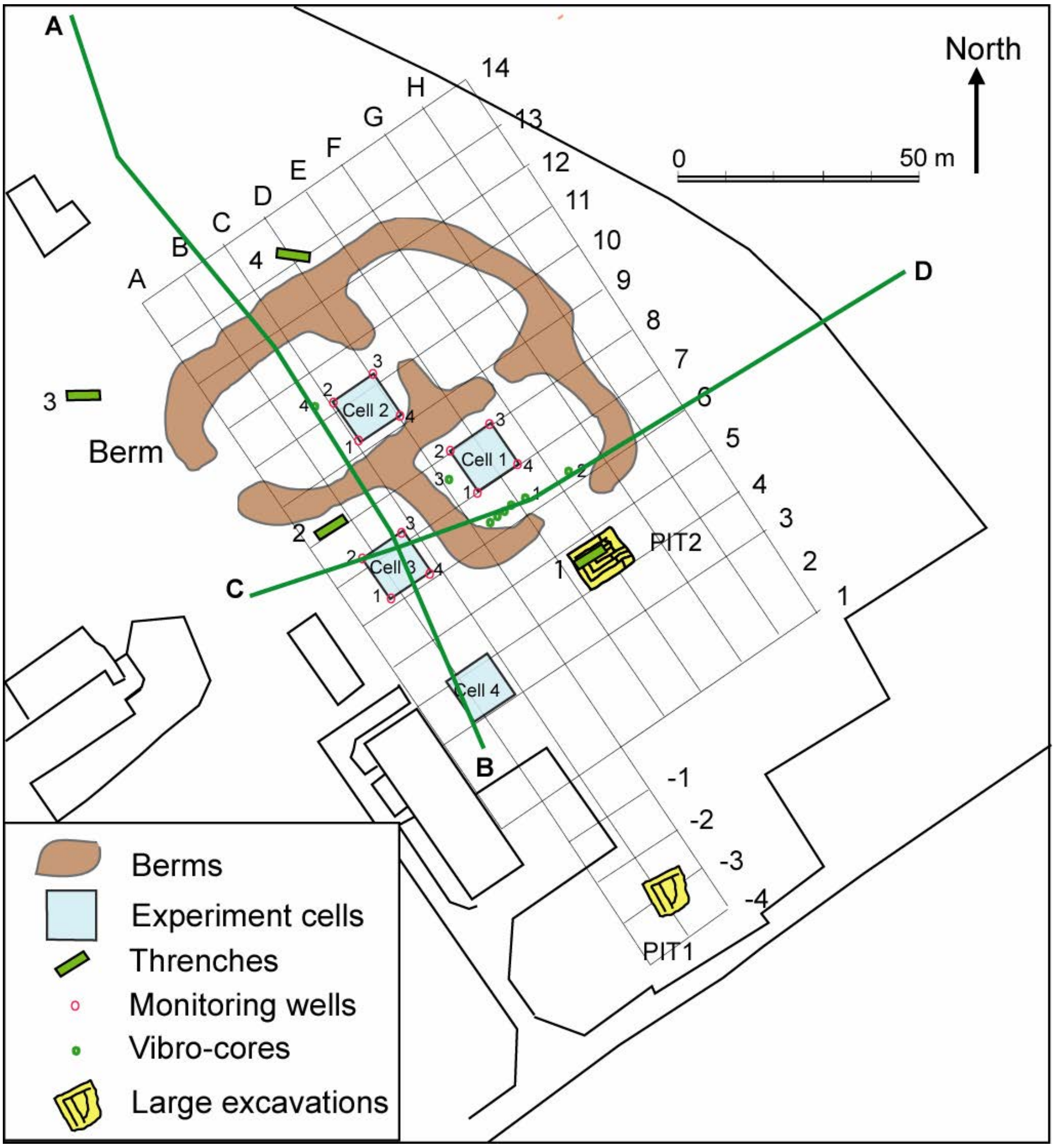

Fig. 4.3 Map over the research area with position of wells, trenches 1-4 and PIT 1 and 2 as well as the four experimental cells. Profile A-B and C-D (Fig. 4.4) was constructed from existing wells.

From the existing wells in the area the thickness of the diamict deposits and the hydraulic head of the groundwater aquifer have been estimated over the site fig. 4.4.

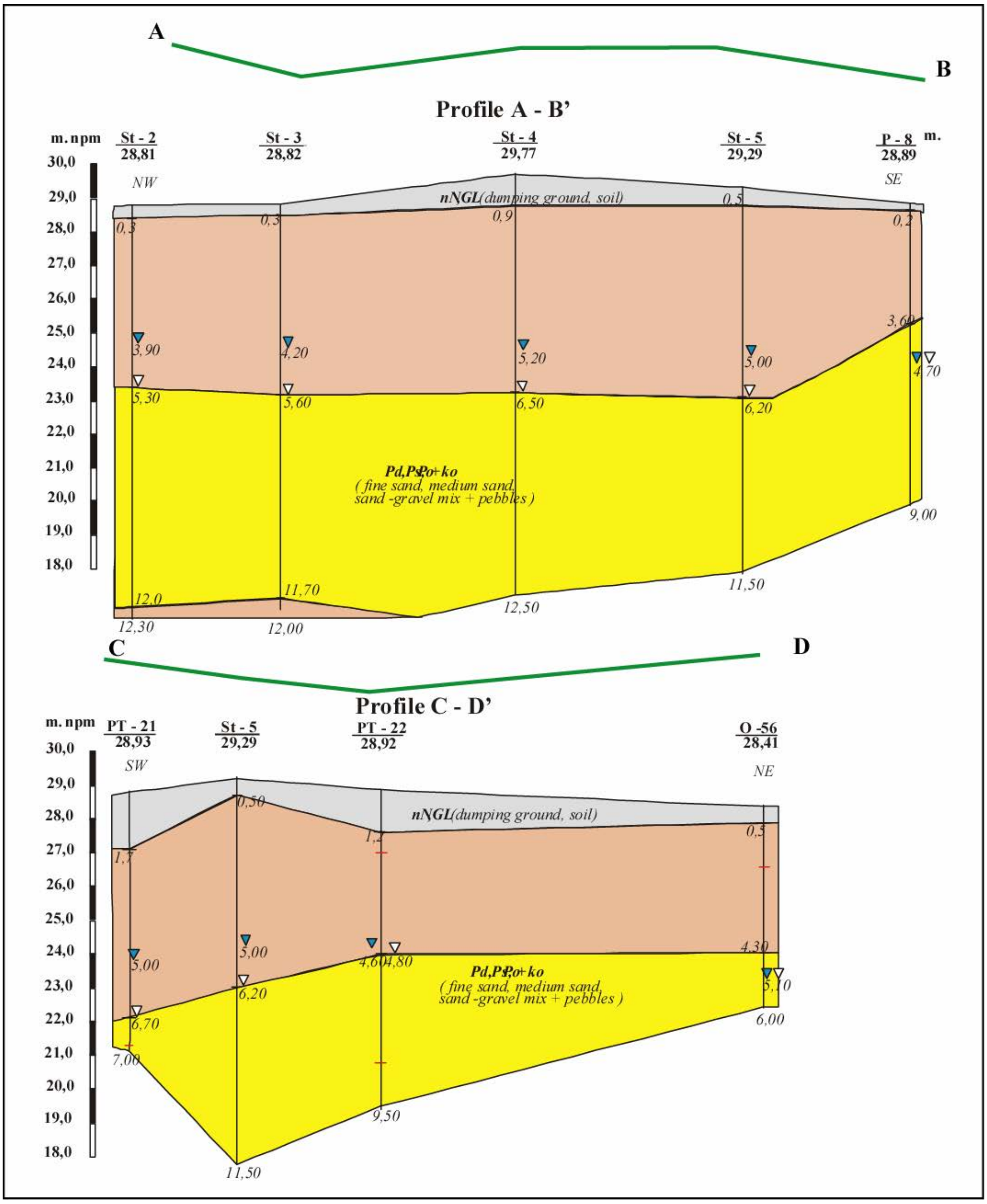

Fig 4.4 Thickness of the glacigene diamict deposits overlaying the sandy aquifer.

Geological characterisation of the sediments along with characterisation of the fractures and other macropores was carried out in the pit, while the trenches and wells were used for describing the spatial distribution of the geological units as well as the fill throughout the site. A grid of the entire site was constructed in order to construct simple reference points for wells and excavations. In that process a great deal of vegetation and concrete foundations were removed in order to make way for the drilling rigs and machinery needed during the construction of the cells.

Hydrogeotechnica has investigated the hydrogeological conditions in the area. They produced a map showing the hydraulic head in the region and as illustrated on fig. 4.5. The hydraulic gradient is directed towards the nearby Lake Miedwie. No investigations of the hydraulic properties of the diamict sediments covering the sandy aquifer has been conducted, and this is accordingly one of the key tasks in this project.

Rys. 2. Mapa hydroizohips zwierciadła wody I-warstwy wodonośnej - lotnisko Kluczewo
stan 04.1996 r.

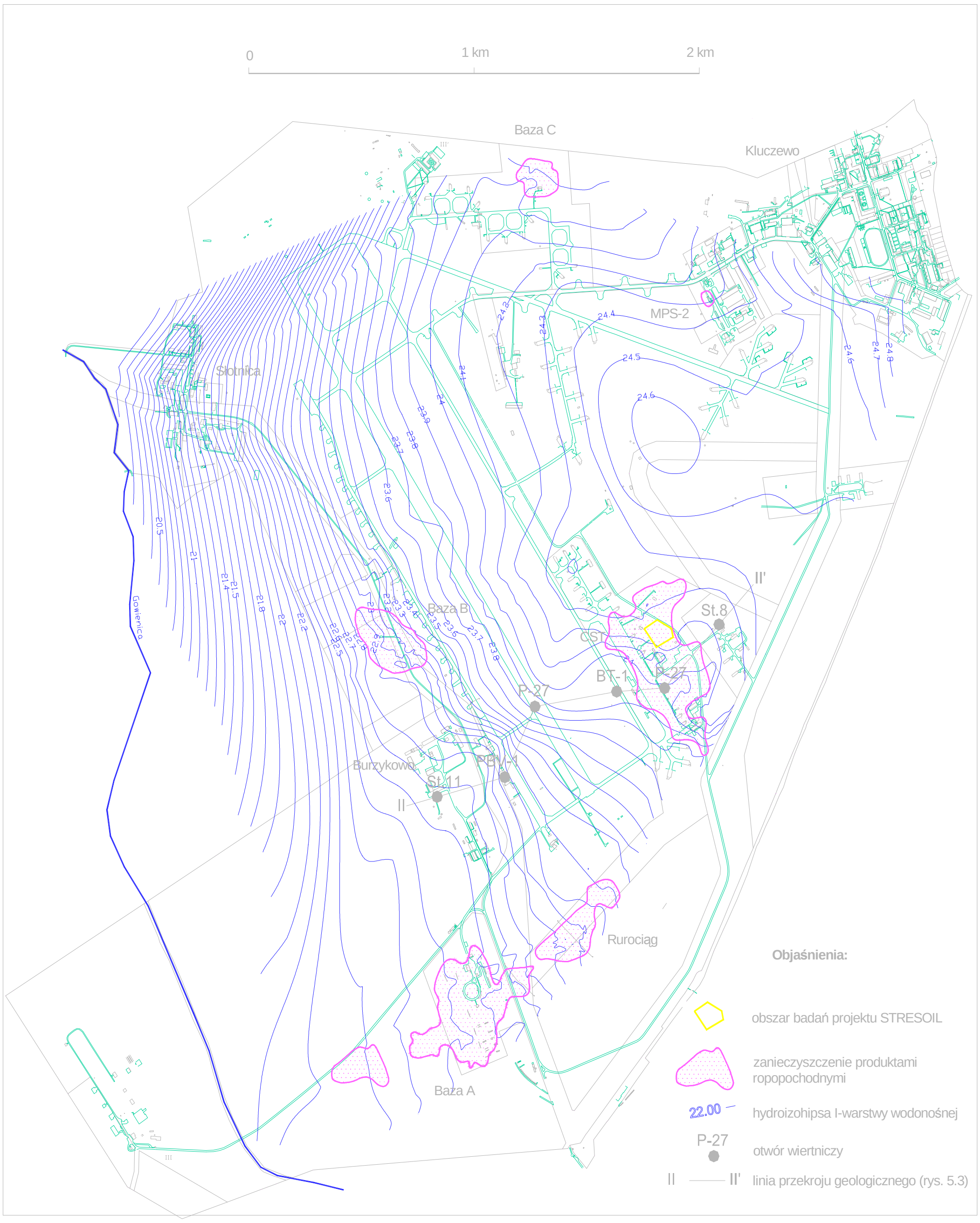

Fig. 4.4 Hydrogeological conditions in the area. As illustrated the gradient of the groundwater table is directed towards west.

5. Methods

Till classification.

The depositional environment is closely related to the formation of fractures and may add important information about the nature and genesis of the fractures. Characterisation and classification of the sediment are accordingly important in order to interpret the origin of the fractures. The classification of glacial deposits was carried out according to methods described by Klint 2001, and a schematic genetic classification of tills is presented in table 1.

A useful systematic descriptions of glacial deposits were proposed by Krüger and Kjær (1999), It consist of a lithofacies code that includes lithology, sedimentary structures, fractures, lateral extension of the diamict unit, contacts, lithofacies, directional elements, genetic interpretation and surface morphology. The investigation of the sediment were thus based on the classical methods listed below:

Kineto-stratigraphic measurements (Berthelsen 1978):
This methodology involve methods for measuring all directional elements reflecting ice movement directions and include:

- Clast fabric analysis of elongated clasts (more than 0,6 cm long and with an a/b-axis > 1.5) were carried out on horizontal faces at different depth intervals as described by Krüger (1994). The fabric is used to classify the diamict sediments along with other features. The primary till-types are basal tills, which includes deformation tills, lodgement tills, glacitectonites and basal melt-out till. These tills are often consolidated with a strong preferred orientation of elongated clasts parallel or perpendicular to the ice-movement direction, in contrast to en-glacial, supra-glacial flow/melt-out till or glacio-marine/lacustrine waterlain tills (drop tills), which have a more random distribution of elongated clasts.
- Measurement of glacial-tectonic deformations are extremely useful for calculating ice-push directions, The orientation of especially fault planes and fold-axis are good ice movement indicators and may also be used to classify the till.
- Orientation of stoss-lee side blocks and striation on ice scoured clasts especially on boulder-pavements, were likewise measured when the occurred, indicating the direction of the ice-movement.

Geo-technical properties.

Diamict deposits exhibit highly variable strength properties. Some geotechnical parameters were accordingly measured to support the lithological descriptions. Intact and disturbed shear strength were measured with a standard shear vane (torvane), and samples (100 cm^3 tubes) were collected in the same positions, for measuring the matrix porosity, water-content and water-saturation in 10-20 cm intervals towards depth.

Bulk samples (2-3 kg) were collected in 0.5-meter intervals towards depth for grain-size distribution analysis and measurement of $CaCO^3$ content.

Grain-size distribution:
Characterise the sediment and add information about the hydraulic properties of the matrix. Sediment samples of the characteristic units were collected for grain-size analysis in the laboratory.

$CaCO_3$ in the matrix: Diamict sediments in this region are generally rich in $CaCO_3$ (15-25%) The $CaCO_3$ dissolves over time and the transition between the $CaCO_3$-rich and $CaCO_3$-poor matrix is also a transition between highly porous (30-45%) and normal porous diamict (25-35%). The consolidation of the diamict also changes abruptly on this transition and the soft highly porous poor matrix enhance bioturbation and root-casts, thus increasing the permeability and decreasing the consolidation of the matrix. This transition is accordingly very important and it was indicated in the field by spraying 10% HCL on the matrix and mark the reactive/non-reactive areas separated by the $CaCO_3$ transition.

Fracture classification

Fractures may be classified as either systematic or non-systematic fractures. The following types of fractures has been recorded in diamict deposits:

Glaciotectonic fractures formed sub-glacially appear generally systematic compared to the ice-movement direction (Fig. 5.1). The fractures are generally restricted to two types of basal tills. Type-A basal tills, which are considered ductile deformed during high pore-water pressure conditions, and Type-B basal till which are considered brittle deformed during well-drained conditions (Benn and Evans 1996).
Type-A tills are normally massive non-fractured, but they may be associated with intrusive sediment filled hydro-fractures, that are either downward injected into the sediments below the till or upward injected from the underlying sediments. These fractures have an overall systematic orientation striking perpendicular to the ice-movement direction with a variable dip down-ice. Sub-horizontal sand filled shear-planes may occur in some A-type basal tills.
Type-B basal tills normally contain up to three fracture systems:

1. One system of sub-horizontal undulating shear-planes, sometimes with a slickenside on the surface, and sometimes sediment filled shear-bands.
2. A second system of straight sub-vertical extension fractures parallel to the ice movement direction.
3. A third system of steep to low-dipping shear fractures oriented perpendicular to the ice-movement direction. They may be developed as two conjugating set of shear fractures or normal faults, and the shape is generally straight, listric or sigmoidal.

Thick tills often have steep dipping shear fractures while thin tills tends to have low-dipping shear fractures.

Basal melt-out tills are normally not fractured, but contains often sand and silt layers, draped over clasts.

Flow-tills may be folded, faulted and fractured due to down and back-wasting processes, when stagnant buried ice melts, but these structures has an overall non-systematic orientation, and a random distribution.

Desiccation fractures form normally vertical polygons, which may be random orthogonal or oriented orthogonal (90^0 between truncations) or hexagonal polygons (60^0 between truncations). The polygons or typically 10-40 cm in diameter and they may be parted into 2^{nd} order polygons 3-6 cm in diameter. They are restricted to fine-grained sediments and will not truncate thick sand-layers or sand-bodies. They are limited downwards by the groundwater table, but “fossil” desiccation fractures may reach below the present groundwater table. In general desiccation fractures continue down to 3-4 meters depth, but they have been observed down to 6.4 meter below the ground surface.

Frost cracks or freeze/thaw fractures forms typically in sandy sediments either as large polygons (ice-wedges) typically > 10 meter in diameter in permafrozen areas, or as minor polygons in connection with frost-cracking in not permafrozen areas (maybe due to differential frost heave). Fine-grained sediments tend to develop pore-ice and segregation ice. This results in compaction and development of sub-horizontal fracture zones dominated by closely spaced micro fractures (2-30 mm spacing). These fracture zones may be highly conductive and facilitate large lateral flow during periods of high groundwater conditions.

The different fracture types and their characteristics are listed in table 2.

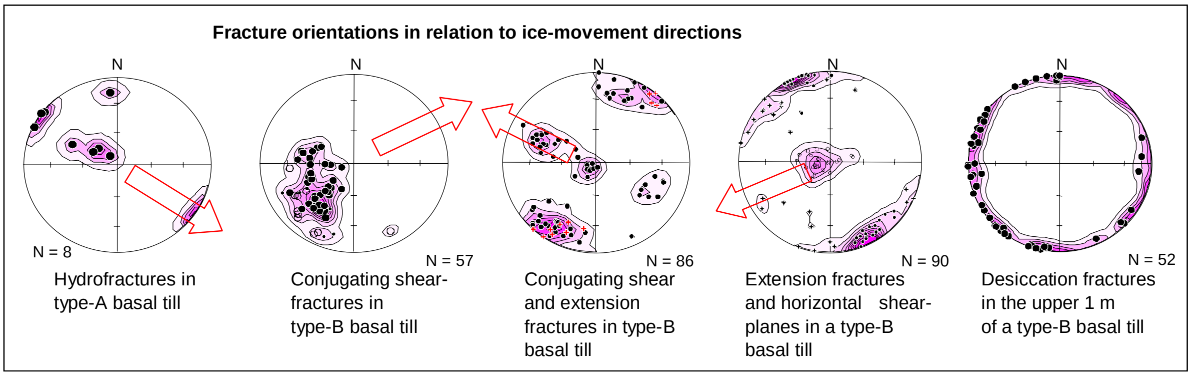

Fig. 5.1 Pole diagram showing the typical fracture orientations in relation to ice-movement directions (red arrow) on selected locations. Note the generally systematic orientation either parallel (extension fractures) or perpendicular (shear fractures) to the ice-movement direction. The occurrence of sub-horizontal shear planes is typical for basal tills, while desiccation fractures are vertical randomly oriented. The data is plotted as poles to the fracture planes on a Schmidt Equal Area lower hemisphere stereographic projection.

Fracture measurement technique.

All the fractures were carefully exposed, by chipping off the surface of the vertical profiles with knife and trowels. The fractures were then measured along a scan-line (ruler) that was attached horizontally to the wall at different depths.

The following fracture data were measured on each 1’st and 2’nd order fracture.

Physical fracture data

Fracture position (placing in relation to a reference line): This parameter is used for reconstructing a profile and calculates fracture spacing and trace frequency. A ruler is pressed against the fracture surface and the position where the ruler cross the reference line is marked.

Fracture order/system: The fractures were classified as 1’st, and 2’nd order fractures. The 1’st order fractures are the dominating fractures cross cutting all other fractures, while 2’nd order fractures are less dominating fractures, sometimes connecting 1’st order fractures without crossing them. If a clear systematic set of parallel fractures can be recognised in the field, it may be given a number as system 1 fractures and another set system 2 etc.

Fracture orientation: The strike (azimuth) and the dip (plunge) of the fracture plane is measured with a compass directly on the fracture surface. The orientation is used for reconstructing the profile, calculate fracture spacing and frequency, identify fracture sets and systems with a preferred orientation and classify the fractures.

Fracture size: The visible minimum size of the fracture is measured, by measuring the trace length of the fractures.

Fracture surface shape: The overall fracture shape (in a m scale) is described as *listric, straight, sigmoidal* or *random..* The shape is used to classify the fractures. This is a qualitative evaluation made in the field, at it is generally useful for characterising fracture systems within the same area.

6. Geological characterisation

The primary purpose of pit no. 1 was to conduct a geological characterisation of the sediment and fractures representative for the area.

Pit no.1 was excavated close to the test site in an area that was considered undisturbed (fig. 4.3). Two sections perpendicular to each other were excavated to a maximum depth of 4.3 m below ground surface. The sections were separated into a number of benches situated 1.8, 2.3, 3.0, 3.5 and 4.3 m below ground surface (fig. 6.1). After excavating the pit, the outermost smeared surface of the vertical sections was removed with scrapers and shovels. Original fractures were generally easily recognised by the colour change in the matrix. The fracture traces in the oxidised matrix are normally grey while they are red in the reduced matrix. All the dominating fractures were then measured along a horizontal scan-line, and described.
Representative samples from six different depth intervals were collected for grain-size analysis and the profiles were carefully examined for characterisation of the sediment.

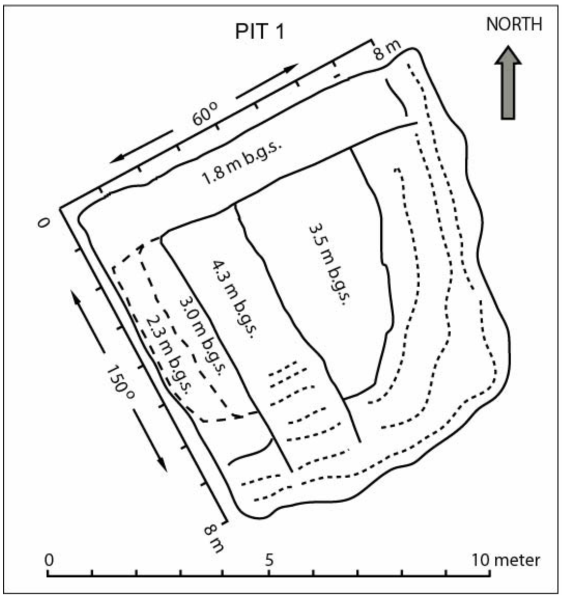

Fig. 6.1. Plane view of pit number 1. The area that is contaminated is clearly marked by the discoloured sediment.

Lithological description and classification of the sediments in pit no. 1

The upper 5-7 meter of the sediments consist of four characteristic units overlaying a regional sandy aquifer consisting of glaciofluvial sand. Fig. 6.2.

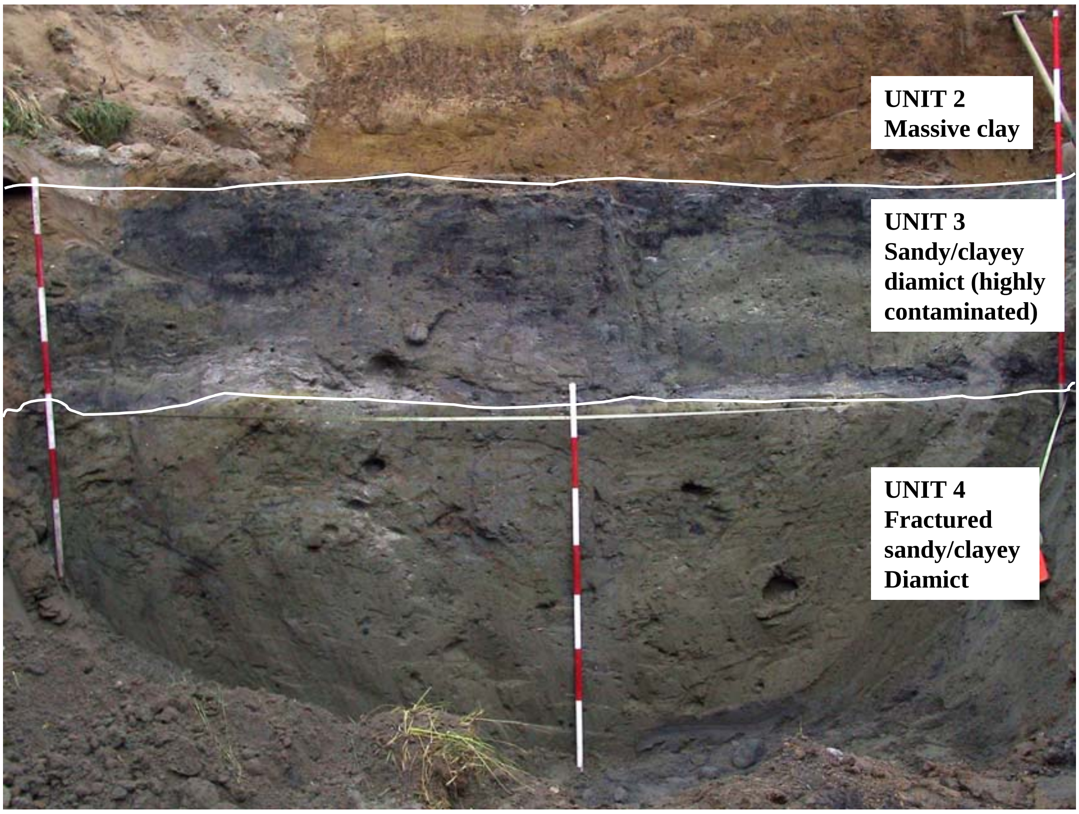

Fig. 6.2 Unit 2-3-4 in pit 1.

Unit 1: 0-0,5 m below ground surface: Fill and topsoil. Remnants of human activity like wires metal parts and other junk is mixed with the soil everywhere in the upper part of the area. A hidden underground tank was situated just south of the excavation.

Unit 2: 0,5-1,75 m below ground surface: Alternating massive clay layers with occasional laminated to massive silt and fine sand layers (fig 6.3). Small pebbles indicate release from floating ice, but no large stones or deformations from grounding icebergs have been observed. The unit is truncated by primarily vertical fractures that are randomly oriented. Root casts are widespread on the fracture surfaces and especially the clay shows a ruptured structure when broken apart. The sediment is classified as waterlain till (glacio-lacustrine clay/silt with drop material) deposited in relative shallow ice-dammed lake.

Unit 3: 1,75-2,6 m below ground surface: This unit is classified as a sandy diamict. It consists of generally poorly sorted material with some clay silt, gravel and few stones. Some of the stones are ice scoured, but fabric analysis shows a random distribution of elongated clasts. Many well sorted sand stringers (fig. 6.4) and some silt draping over clasts and slightly deformed sand stringers indicate deposition in an aquatic environment, with occasional deformation of the sediments. The diamict is accordingly related to debrisflow-processes alternating with sub-aqueous sedimentation in a lake and the sedimentary environment is very close to the glacier margin. The till is accordingly classified as flow-till. This unit varies in thickness from 60 cm to 120 cm. Unit 3 is highly contaminated and forms clearly a higher permeable layer between two massive units. Contamination has apparently migrated laterally in this layer.

Unit 4 2,6-5,15 m below ground surface: The till is silty, strongly sandy with some gravel and stones, it becomes sandier near the lower base. The till is firm and fractured in the upper part (fig. 6.5). The fracture density is high near the base and decreases towards depth. Approximately 2 m under the top of the till the matrix becomes softer and the fractures disappear. The lowermost part of the till appears accordingly soft and massive. Most of the fractures contain contamination (black cover) while matrix smell strongly. This unit is classified as a type A- basal till at the base, gradually transforming into a type B-basal till in the uppermost part (See table 1). Clast fabric and fracture characteristics indicate that the till was deposited below a glacier transgressing the area from northwest.

Unit 5 below 5,15 meter: Unit no. 5 consists of glaciofluvial well-sorted sand that is strongly contaminated with free phase jetfuel.

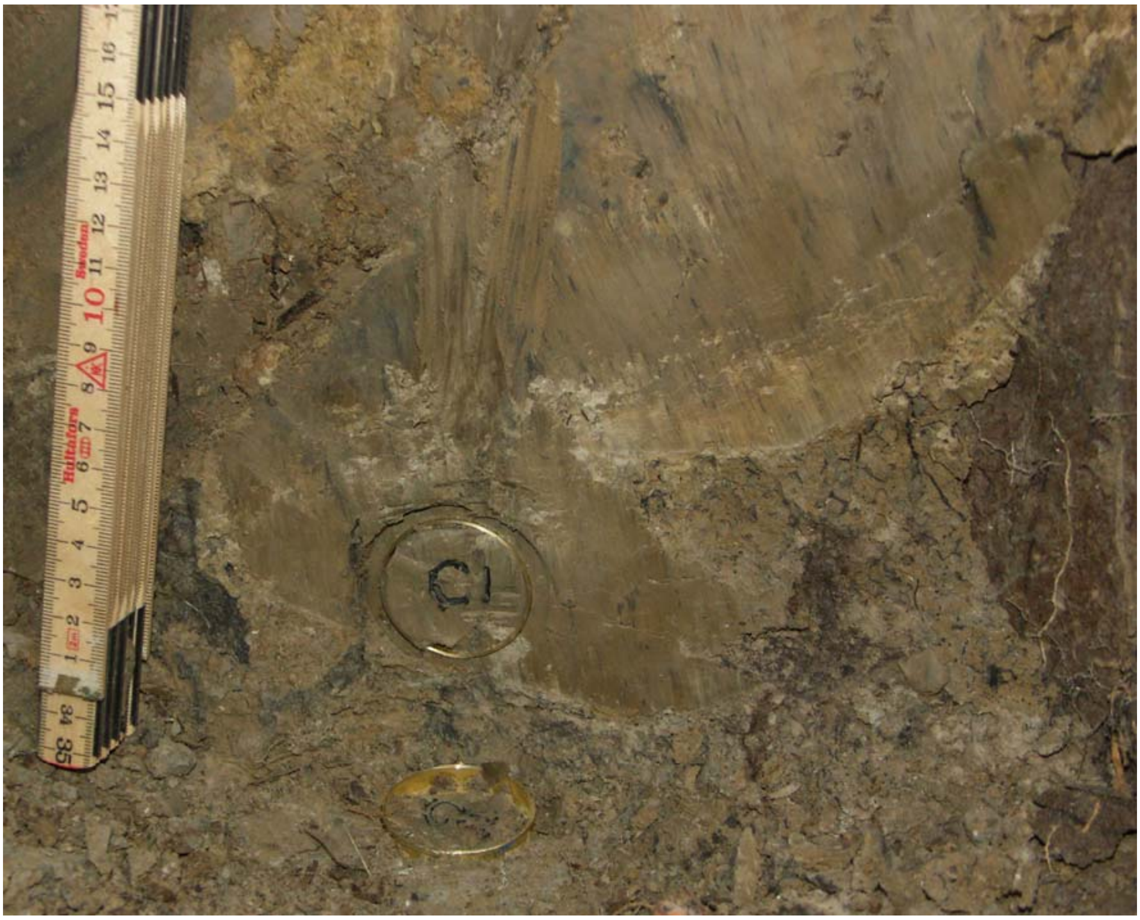

Fig. 6.3: Unit 2. Massive Clay with layers of laminated silty-fine sandy deposits.

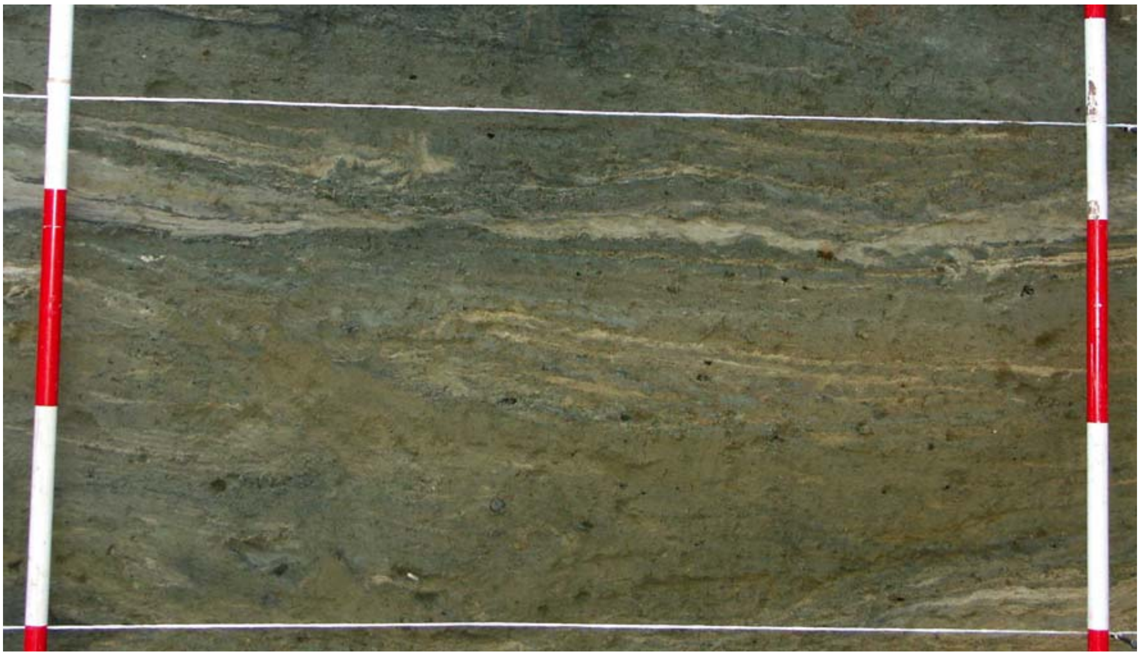

Fig. 6.4: Unit 3 Section is 1 x 0.5 m. Note the layering and the thin sand stringers.

Fig. 6.5: Unit 4, Fractured basal till. Note the discolouring indicating fractures with contamination and the red iron oxide staining on non-contaminated fractures.

Grain-size distribution

The distribution of the grain-size was measured in all the units except unit 5, which was never exposed in the pit. Unit 2 had a larger variation with massive clay in the upper part and silty, fine sanded parts in the lowermost part.

Both curves for unit 3 and 4 shows a classic shape for diamict glacigene deposits.

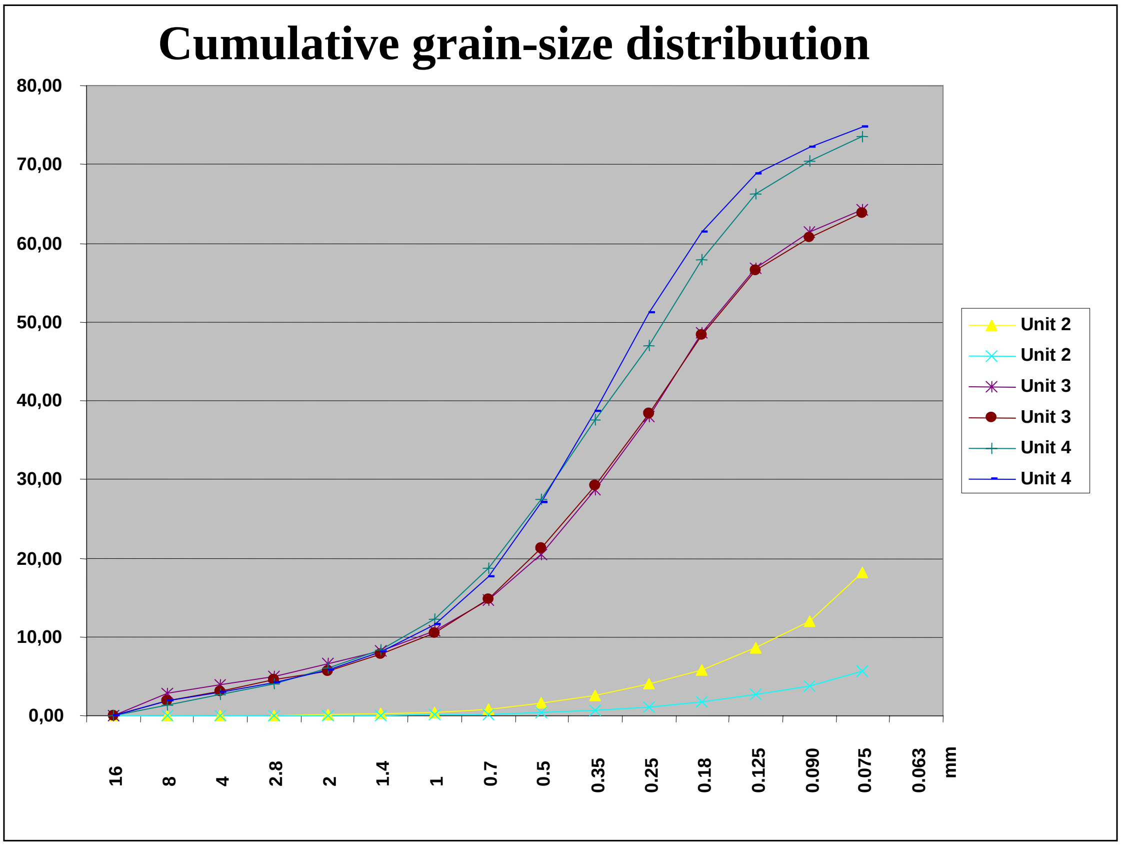

Fig. 6.6: Grain-size distribution in the different units shows generally small variations within the units. Unit 4 is the sandiest unit while unit 3 is slightly more clayey. Unit 2 (lacustrine clay) has a very high clay/silt content, but also a rather large variation.

Fracture classification

Fractures were measured along two 4-m long horizontal reference lines situated 1 m below ground surface in the lower part of Unit 2 and 3 m below ground surface in the upper part of unit 4. No fractures were observed in Unit 3. The orientation of the fractures is illustrated on fig. 6.7.

Unit 2

The fractures in Unit 2 were predominately vertical fractures with a random strike. 55 fractures were recorded on a 4 m section which gives an average fracture trace frequency of

13.8 fracture traces/m or an average distance between the fractures on 7 cm. The fractures had a generally undulating rough surface character with multiple root-casts and earthworm burrows on the surface, thus forming a network of connected macropores. The fractures ended towards the underlying sandy unit, and they formed a clear polygonal pattern with 10-15 cm wide 1st order polygons that were further separated into minor 2nd order polygons 4-7 cm wide.

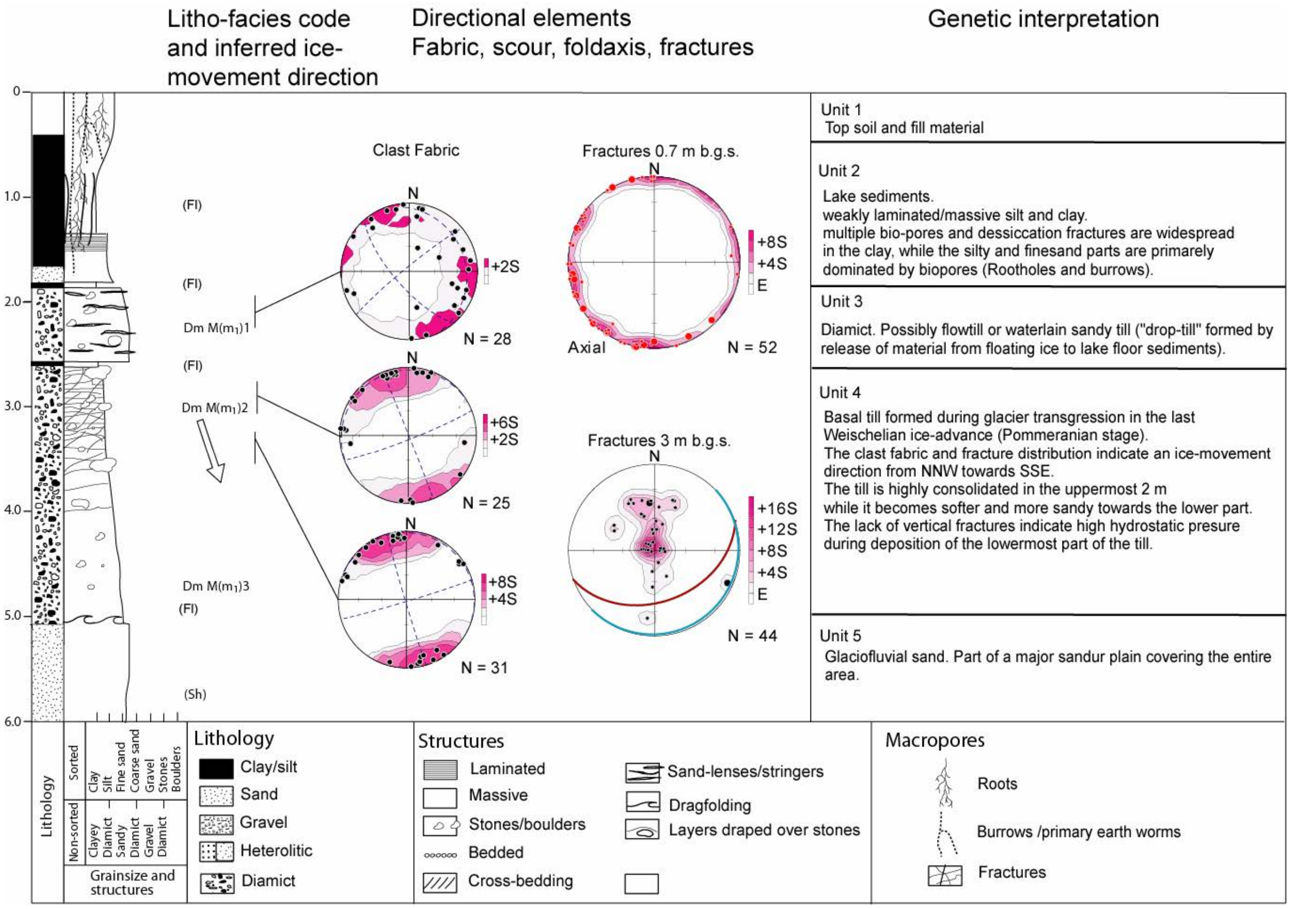

Fig. 6.7: Lithological log from excavation no. 1. Description and facies-code after Krüger and Kjær, 1999.

The nature of the fractures made it clear that the fractures can be classified as desiccation fractures (table 2). The clay matrix had furthermore a ruptured structure with mm size micro cracks. These fractures had a light grey colour with a silty surface texture and a random orientation. The structure is typical of that formed by freeze-thaw processes during formation of pore-ice and segregation ice. Such a structure clearly increases the permeability of the matrix.

These fractures really contribute to the hydraulic conductivity of the clay, but the largest and most important contribution to the bulk-hydraulic property of unit 2 may properly be related to biopores within the matrix. Earthworm holes were counted on 20 x 20-cm horizontal planes and fig. 6.8 shows the distribution of earthworm burrows and fractures towards depth, while root-casts are registered using image analysis of fracture surfaces (fig. 6.9).

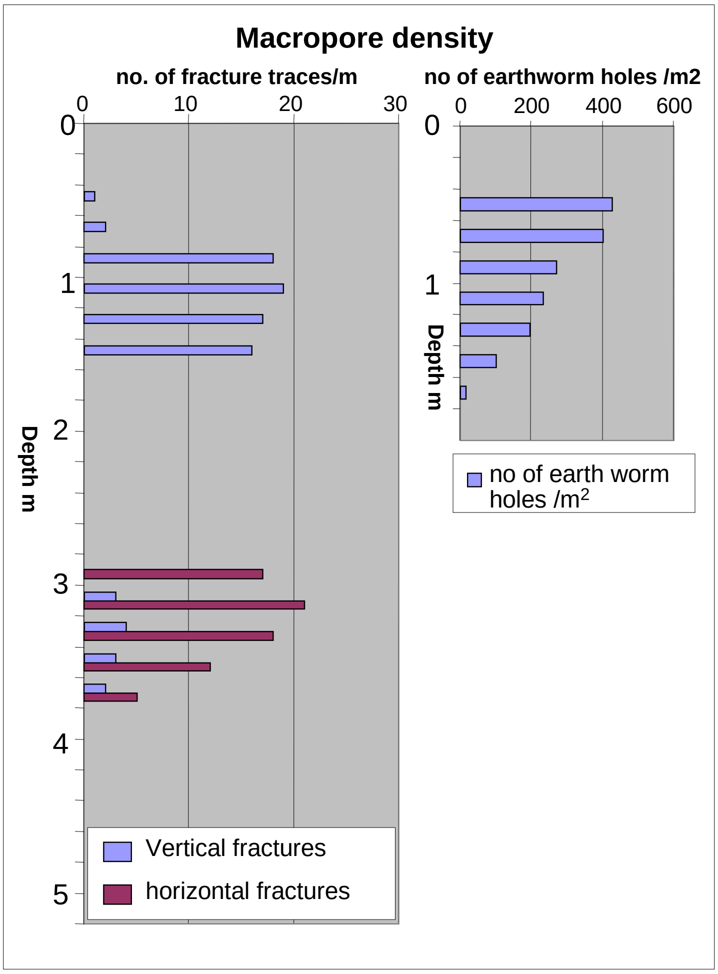

Fig. 6.8: Fracture density and bio-pore distribution in Pit 1.

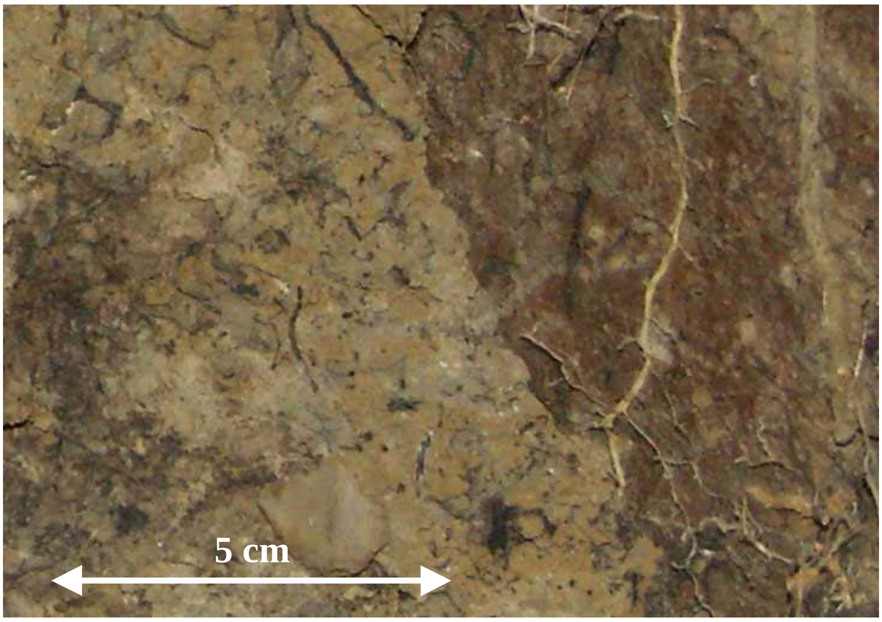

Fig 6.9: Root-casts on the surface of desiccation fractures. Note how matrix is penetrated by bio-pores.

Unit 4

Unit 4 is highly fractured in the uppermost 1.5-2 m. 43 fractures were recorded and described along 4-meter profile at 3 meters depth. As illustrated on the stereographic projection fig. 6.7 and on the photo fig. 6.5 two primary systems of fractures dominate.

System 1 consists of sub-horizontal fractures and system 2 consists of oblique fractures striking 80° with a gentle dip of 30-45° towards south east. The fractures are formed perpendicular to the ice-movement direction recorded from the fabric and scour mark analysis. The dip is generally down-ice and the fractures may those be classified as glaciotectonic fractures formed by the loading and shearing from a transgressing glacier. The spacing between the horizontal fractures are approximately 3-4 cm in the uppermost part and decreasing towards depth and are gradually transformed into a fissility 1.5 meter below the top of unit 4.

The system 2 fractures are larger and sometimes with a thin sand filling. The average fracture spacing of the system 2 fractures are between 15-20 cm and they reach approximately one meter into unit 4.

Conceptual macropore distribution model

Based on the measured field data a conceptual geological model representative for the site has been defined (Fig 6.10). The thickness variation of the different units is illustrated on Fig. 6.11.

A conceptual fracture model with detailed description of the aperture of the different fracture systems is almost finished (due at the end of August 2005) and the individual geological models for the three tests-cells are currently being updated with the new well data from the stimulation activities achieved during WP2.

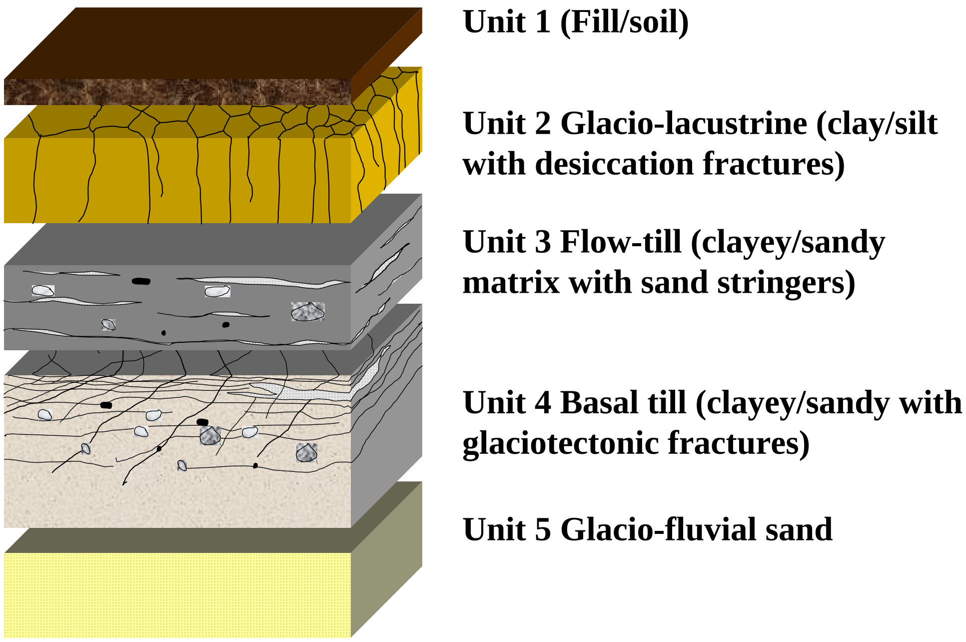

Fig. 6.10: Conceptual geological model with the 5 units and typical distribution of macropores/fractures within the different units. As illustrated the fractures in unit 2 are predomi-

nantly vertical desiccation fractures, while the fractures in unit 4 are dominated by sub-horizontal shear fractures and oblique dipping conjugating shear fractures. These fractures are classified as glaciotectonic fractures formed by loading and shearing from overriding glaciers.

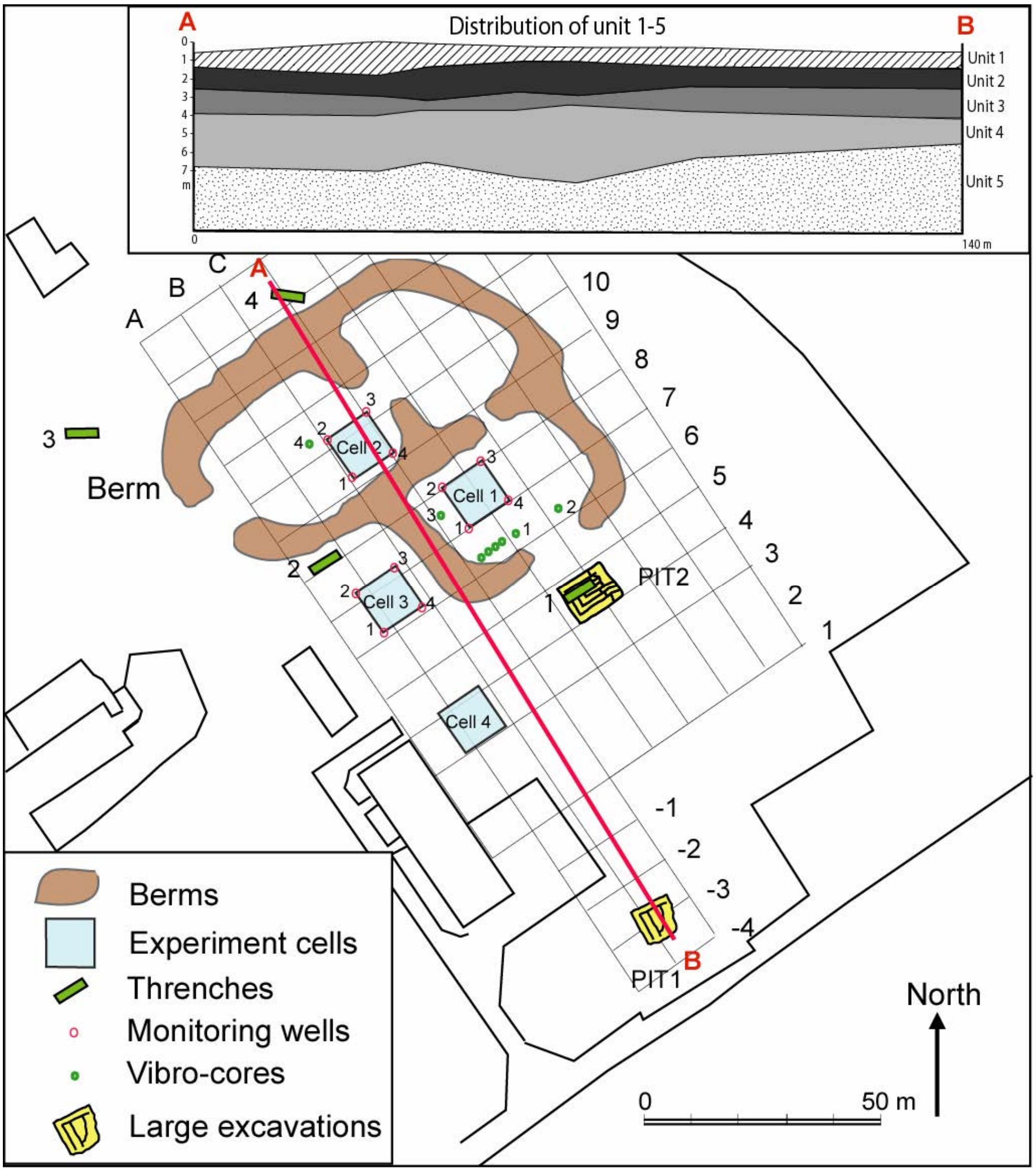

Fig. 6.11: Spatial Distribution of Unit 1-5 across the Site.

7. Core and soil sampling

The main purpose of pit no. 2 was to collect samples of contaminated soil and describe the spatial distribution of contamination in the different units and in the fractures, and secondly to collect samples for calculation of hydraulic parameters. Pit no.2 was excavated in the period 27-30 August 2004, close to the actual testsite in order to be representative for the test cells (fig. 4.3).

The pit was excavated in the shape of an U to a maximum depth of 5 m below ground surface. The sections were separated into a number of benches situated 1, 2.3, 3.5 and 5 m below ground surface (fig. 7.1). After excavating the pit, the outermost smeared surface of the vertical sections was removed according to the same methodology that was used in pit no. 1

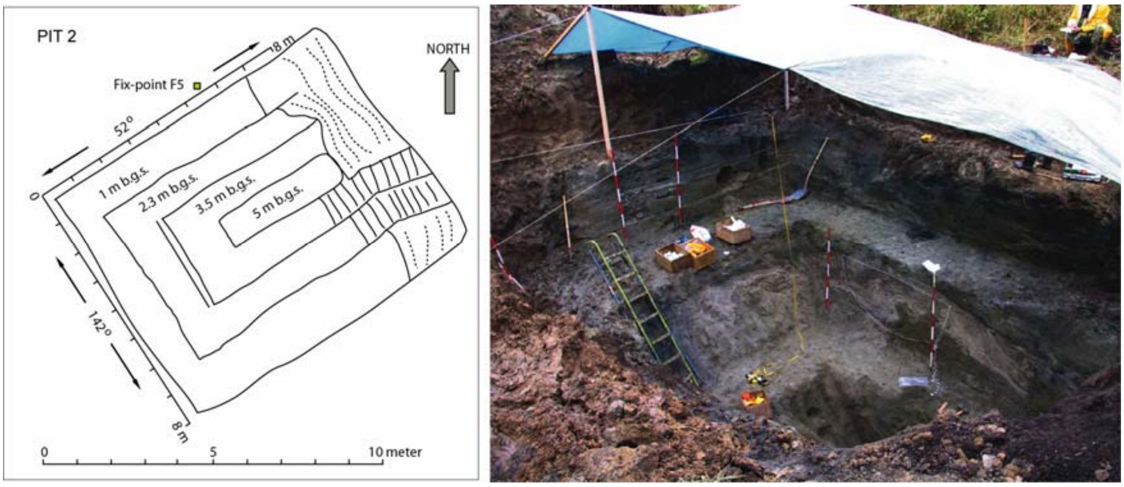

Fig. 7.1: Pit. No 2.
A number of vertical and horizontal sections were carefully cleaned and photographed for image analysis of colour distributions that may be linked to distribution of contamination.

Lithological description and classification of the sediments in pit no.2

Pit no. 2 had generally the same geological units as described in pit no.1. The main difference was the thickness of the individual units as well as the occurrence of a major sand lens in the uppermost part of unit 4. The distribution of the lithology is illustrated on fig. 7.2

Unit 1 0-0,4 m below ground surface: Fill and topsoil. Remnants of human activity like wires metal parts and other junk is mixed with the soil everywhere in the upper part of the area. An old excavation down to 2.5 meter below ground surface was situated in the southern part of the pit

Unit 2 0,4-1,25 m below ground surface: Alternating massive clay layers with occasional laminated to massive silt and fine sand layers. The unit is truncated by primarily vertical fractures that are randomly oriented. Root casts are widespread on the fracture surfaces and especially the clay shows a ruptured structure when broken apart.

Unit 3 1,25-2,4 m below ground surface: Flow till consisting of generally poorly sorted material with some clay silt, gravel and few stones. Many well sorted sand stringers with occasional deformation of the sediments. Unit 3 is highly contaminated and forms clearly a higher permeable layer between two massive units. Contamination has apparently migrated laterally in this layer.

Unit 4 2,4-5 m below ground surface: Basal till. The till is silty, strongly sandy with some gravel and stones, it becomes more sandy near the lower base. The till is firm and fractured in the upper part. The fracture density is high near the base and decreases towards depth. A sand-lens near the transition between the unit 3 and 4 were intensely deformed with development of classical drag folding. Measurements of fold-axis orientations indicate an ice-movement from NNE.

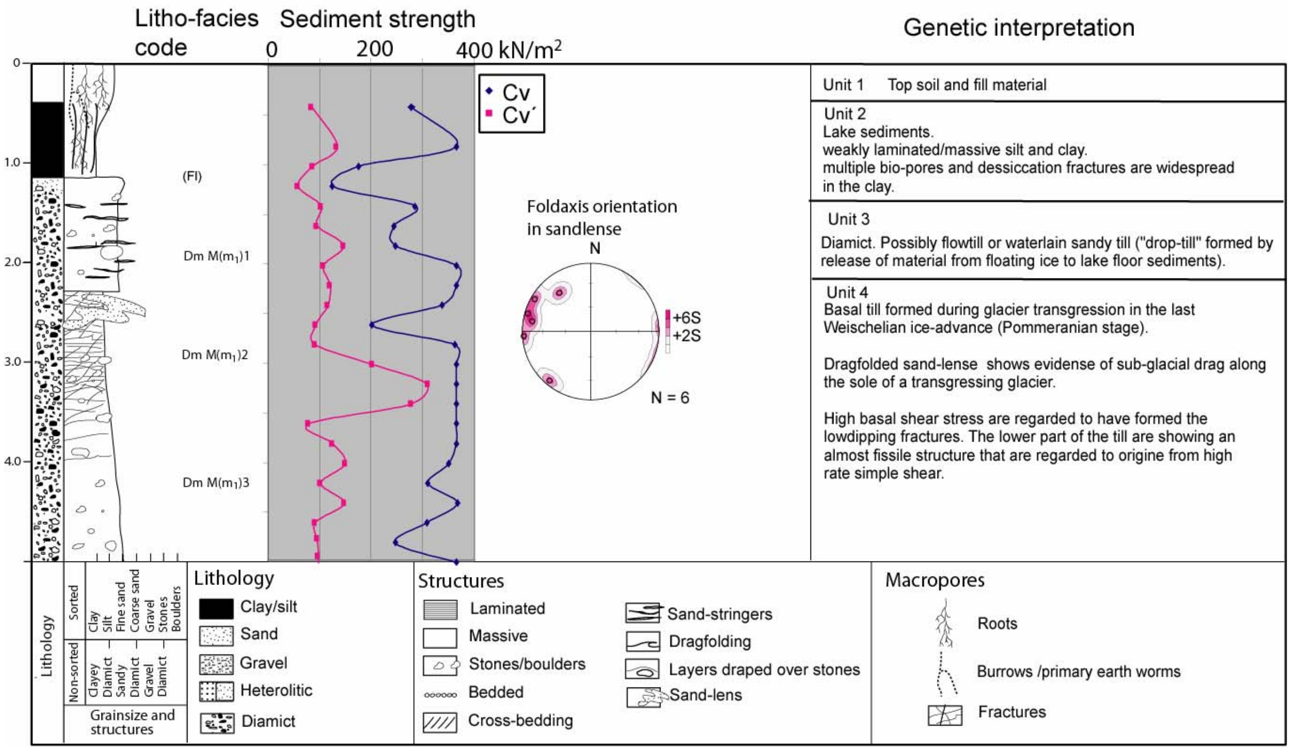

Fig. 7.2 Lithological log showing the distribution of unit 1-4 in pit no. 2. Intact and disturbed shear strength were measured in 20 cm interval from the surface to 5 m depth with a standard shear vane (torvane) by HGT. It shows that the unit 2 is very firm (due to desiccation of the clay, while unit 3 is softer especially in the sandy regions. Unit 4 is generally firm, but becomes softer downwards. A sand lens in the upper part also exhibit low shear strength values.

Collection of samples

The following samples were collected.

Core samples

- 52 core samples of intact sediment were collected for measurement of transport properties laboratory experiments by ICE-HT.
- 25 core samples were collected for measuring geotechnical properties by HGT.

Bulk samples

10 x 2-kg bulk samples of the sediment were collected by GEUS for the analysis of petrologic and textural properties.

Intact samples

5 contaminated intact samples were collected for impregnation and image analysis of micro-morphological features (Klint and Tsakiroglou 2000). The samples represent examples of dominant fractures at different depths, thus representing the variation of pores in the three till units (unit 2,3,4). A smooth face perpendicular to the fracture was cleaned and a stainless steel box (Kubiena box, (15 x 8 x 5 cm), with a removable top and bottom lid, were placed perpendicular to the fracture. While very carefully removing the sediment along the outer side of the box, the box were gently pushed further into the matrix, until a small monolith containing a fracture was excavated.

A sketch of the macrostructure's in the sample was drawn, and the orientation and position of the box and fracture were measured. Finally the box was sealed airtight with plastic-bags and tape and placed in a refrigerator at 5 C^{o}.

Soil samples for Pollute Eval.

Finally an extensive sampling of contaminated soil and water samples was carried out by IFP for the mapping of the fate and distribution of contamination in the matrix and in the fractures. The terrain version of the Pollute Eval apparatus was involved in this part in order to characterise the spatial jet fuel distribution in the soil with on site analyses. About 100 to 150 Pollut Eval analyses were carried out on site by IFP (See annex 1 table 3).

8. Determination of the spatial distribution of NAPL over the site

The analytical results of the different soil and oil phases sampled at the Kluczewo site showed clearly a contamination with Jet Fuel. The chromatogram presented in Fig. 8.1 is very characteristic for a Jet Fuel that has been subjected to a very limited weathering.

The figure shows that the hydrocarbon mixture fund in the Kluczewo site has a normal behaviour concerning the equilibrium with water from a thermodynamically point of view. The concentrations, expected to be found in water according Raoult's law after a diphasic contact, are quite in line with those practically found. This allows setting up a complementary analytical strategy involving soil extraction and soil leaching. Further more, since the soil leaching capacity of a soil is a very important parameter in term of risk assessment regarding the ground water, this value will be a very useful tool to evaluate the success of the remedial action undertaken.

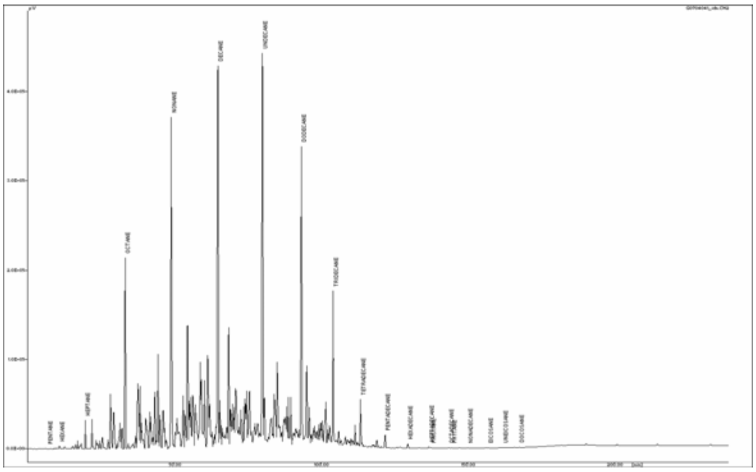

Fig. 8.1 GC chromatogram of the Kluczewo Jet Fuel

Components	Concentration theoretical [µg.L-1]	Concentration expérimental [µg.L-1]
BENZENE	15	22
TOLUENE	78	106
ETHYLBENZENE	678	815
META-XYLENE	755	903
PARA-XYLENE	356	485
ORTHO-XYLENE	1 021	1 144
N PROPYLBENZENE	404	195
1,2,4-TRIMETHYLBENZENE	809	195
1,2,3-TRIMETHYLBENZENE	502	331
NAPHTALENE	80	374
TOTAL AROMATICS	4 697	4 571

Table 1. Hydrocarbon concentration in the water, experimental result and calculation results according to Raoult's law based on Carburane results.

Another very important characteristic of the Kluczewo site is the heterogeneity of the pollution distribution in the soil. This heterogeneity is illustrated in the Fig.8.1

Such behaviour of the pollution is due to the geological situation with low matrix permeability and high fracture conductivity.

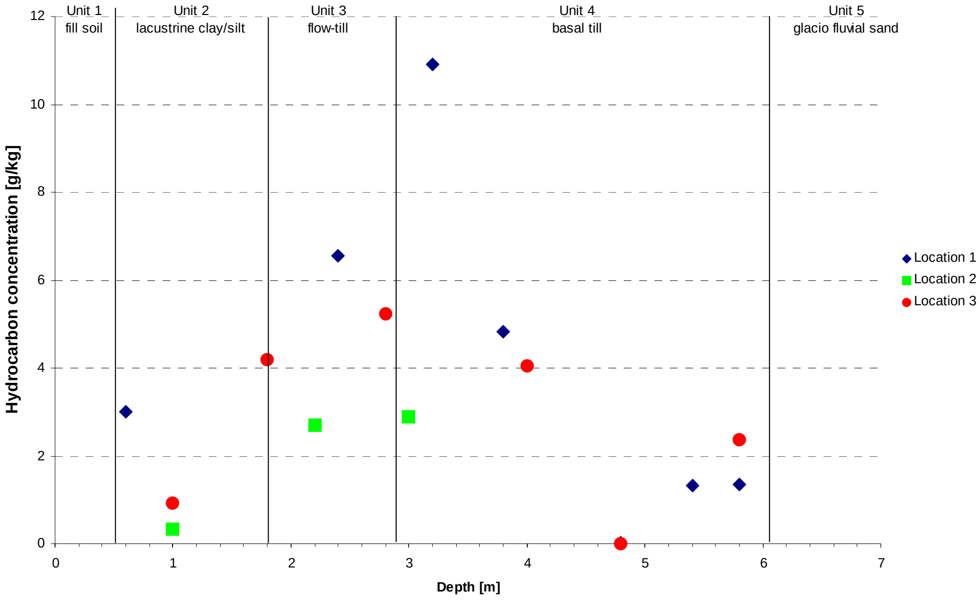

Fig. 8.2 Pollution distribution, Pollut Eval analysis

Due to the volatility of the polluting hydrocarbons and the nature of the soil, the samples have to be prepared and conditioned on site for all the further analytical characterisations that will be done in the laboratory.
The greatest care will be given to limit the loss of the volatile fraction for both the water leaching and the exhaustive extraction of the hydrocarbons present in the soil samples.
The soil characterisation implemented to assess the treatment progress will be based on the analysis of hydrocarbons present in the soil and the determination of the water soluble hydrocarbons after soil leaching.

Soil Leaching:

The leaching potential of soil samples will be determined immediately after they have been taken out of their natural environment. Therefore approximately 30 to 35 g of soil (precisely weight) will be immediately stored in 250 ml glass flasks (Schott, with red GL 45 screw caps equipped with Teflon coated silicone septum) and than filled with distilled containing 1 g/L $HgCl_2$. A mass of 30 to 35 g of humid soil will insure about 25-g dry material corresponding to 10% of the water volume. The presence of $HgCl_2$ in the distilled water will ensure that no biodegradation of the hydrocarbons may occur during the leaching and the transport to the laboratory.

Hydrocarbon extraction from the soil

The hydrocarbons will be extracted from the soil with Dichloromethane. The extraction is realised on site. The flasks are prepared with 40-ml solvent in the lab, and approximately

30 to 35 g of soil (precisely determined) is weight in this flask immediately after sampling in order to avoid any volatilisation of pollutants. The extraction solvent contains two internal standards (1,1,1-Trichloroethane (1,1,1-TCA) and (nC20)).
The flasks will then be shipped to the laboratory.
Appendix 3 gives a list of soil samples received by IFP and analysis types done on the samples. This list does no take into consideration the Pollut Eval analyses realised on the soil. About 100 to 150 Pollut Eval analyses have been undertaken until now in the frame of the Stresoil project.

Microbiological characterisation of the site

The analytical results of the different soil and oil phases sampled at the Kluczewo site showed clearly a contamination with Jet Fuel. The chromatogram presented in Fig. 8.1 is very characteristic for a Jet Fuel that has been subjected to a very limited weathering.
The preliminary results concerning the biodegradation of the pollution (fig. 8.3) showed that competent micro flora are present in the soil. These data also indicate clearly that the main limiting factor for the biodegradation is the accessibility of oxygen to the bacteria present in the soil of the vadose zone.
Due to these reasons we assume that the biological treatment of the pollution present in the vadose zone of the Kluczewo site should be a successful treatment measure if oxygen could be distributed in the contaminated matrix.

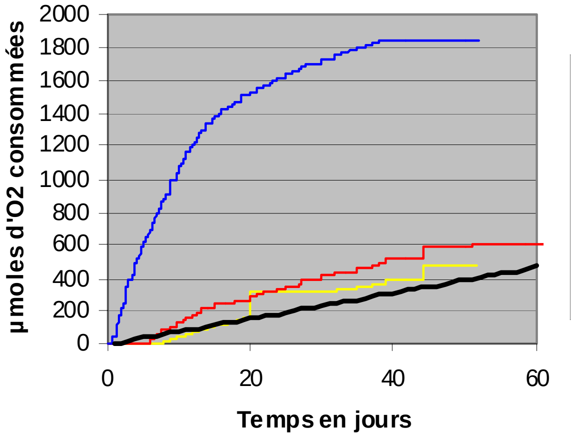

Fig. 8.3: Oxygen consumption during different biodegradation experiments with Kluczewo soil samples undertaken in different conditions.

9. Summary

1. A general geological model has been established for the entire area based on existing data, and a detailed local geological model has been established for the experimental site.

2. An area in the eastern part of the airport was selected for the experiments. A great deal of data exists for this area and it has good logistics (electricity, water roads etc.).

3. Based on the investigations in the two pits a preliminary conceptual geological model has been constructed. The investigations showed that the glacial deposits were not consisting of one till unit, but actually topsoil + three different till units overlaying a sandy aquifer. The different units is classified as:

- Unit 1. Topsoil and fill.
- Unit 2: 1-2 m thick fractured glacio lacustrine clay/silt with ice-dropped gravel/stones. (waterlain clay till).
- Unit 3. 1-1.5 m thick a sandy flow-till.
- Unit 4. 3-4 m thick fractured basal till.
- Unit 5: 6-10 meters of meltwater sand.

4. The hydraulic head of the aquifer is situated between 4.5 and 5 meter depth in most of the area. The investigations showed furthermore that the different units were rather homogeneous distributed throughout the area.

5. From the field investigations, a detailed classification of the fracture systems in the area was carried out, and quantitative fracture properties were calculated for the individual fracture systems. Other features, which could increase substantially the permeability of the sub-surface, such as root-holes and burrows were described as well. The nature and origin of the individual fracture systems was determined and formed the basis for an evaluation of the general fracture distribution in the areas.

6. 52 core samples of intact sediment were collected by ICE-HT for laboratory experiments and measurement of transport properties. A database with the general distribution of the contamination based on existing data was established by IFP for describing the macro-scale distribution of NAPL in the area. Selected soil samples and water samples were subjected to detailed laboratory analyses with chromatographic techniques in order to determine quantitatively the concentrations of NAPL compounds in the pit. The analytical results of the different soil and oil phases sampled at the Kluczewo site showed clearly a contamination with Jet Fuel that has been subjected to a very limited weathering.

7. The preliminary results concerning the biodegradation of the pollution showed that competent micro florae are present in the soil. These data also indicate clearly that the main limiting factor for the biodegradation is the accessibility of oxygen to the bacteria present in the soil of the vadose zone.

10. References

Benn, DI., Evans, DJA., 1996. The interpretation and classification of sub-glacially deformed materials. Quaternary Science Reviews, 15, 23-52.

Berthelsen, A., 1978. The methodology of kineto-stratigraphy as applied to glacial geology. Bulletin of the Geological Society of Denmark, 27, Special Issue, 25-38.

Houmark-Nielsen M. and Kjaer K.H. 2003. Southwest Scandinawia, 40-15 kyr BP. Palaeogeography and environmental change. J. Quaternary, Sci., Vol. 18 pp. 769-786.

Klint, KES., Tsakiroglou C.D., 2000. A New Method of Fracture Aperture Characterisation. In Protection and Restoration of the Environment V. Proceedings of an International Conference, Thassos, Greece, Ed: V.A. Tsihrintzis, G.P. Korfiatis, K.L. Katsifarakis, A.C. Demetracopoulos. 1, 127-136.

Klint, K.E.S., 2001. Fractures in Glacigene Diamict Deposits; Origin and Distribution. Ph.D.-thesis. Geological Survey of Denmark and Greenland., Report, 129, 1–40.

Krüger, J., 1994. Glacial Processes, Sediments, Landforms, and Stratigraphy in the Terminus Region of Myrdalsjökull, Iceland. (Two Interdisciplinary case studies). Folia Geographica Danica TOM.XXI. 233 p.

Krüger, J., Kjær K.H., 1999. A data chart for field description and genetic interpretation of glacial diamict and associated sediments - with examples from Greenland, Iceland and Denmark. Boreas, 28, 386-402.

Appendix 1

Classification of Fine-grained Diamict Deposits		
Subglacial till (Basal Tills)	**Deposition process**	**Special characteristics**
Lodgement till Type A Type B	Lodgement till is deposited by plastering and deformation of glacial debris from the sliding base of a moving glacier A-type: Dominant ductile deformation probably during saturated conditions. B-type: Dominant brittle deformation probably during unsaturated conditions.	Generally massive, Ice scoured stoss-lee side blocks. Boulder-pavements. Large content of exotic material (not locally derived). A-type Generally low to medium strength, massive matrix with occasional water escape structures and intrusion of hydrofractures into the subsurface. Medium/strong fabric. Dragfolding. B-type: High strength, massive matrix, generally strong clast fabric. Often Low dipping fissile shear zones, systematic fractured or faulted.
Deformation till Type A Type B	Deformation tills are formed as a result of pure deformation of the substratum under the sliding base of a moving glacier.	Large content of locally derived material. Same deformation structures as the lodgement till. Type A (Ductile deformation) Low strength diletant till. Type B (brittle deformation) High strength non-diletant till.
Glacitectonite	A glacitectonite is a glacial breccie formed as a result of basal squeezing and crushing of the substratum by a moving glacier.	Medium-high strength, highly deformed (brecciated) transition towards underlying substratum primarily consisting of the still recognisable basement material mixed with till.
Subglacial melt-out till	Melt-out till is deposited by a slow release of glacial debris from the sole of a stagnant glacier by subglacial melting.	Low strength. Very strong clast fabric, layers draped over clasts. Clasts are less rounded than in the lodgement till. Often imbedded rafts of substratum.
Supraglacial Tills	**Deposition process**	**Special characteristics**
Flow till	Flow-tills derive from any glacial material that is released from glacier-ice or from freshly deposited till and which is redeposited by gravitational processes.	Low strength. Varied clast fabric, sometimes layered with inclusions of glaciofluvial sediments. Random orientation of foldaxes fractures and faults. Sometimes stacked sequences of debris-flows.
Supra glacial melt-out till	Derive from any glacial material that is slowly released from glacier-ice without being redeposited	Low strength. Sorted and unsorted sediments. Small basins with primary sedimentary structures, sometimes with small-scale faulting from collapse after melting of buried ice.
Waterlain tills	Glaciers and icebergs floating in lakes or oceans will release drop material to the sea or lake-floor sediments, and sometimes deform them directly by grounding. Turbidites occurs occasionally.	Glacio-lacustrine: Usually clay-rich, thick sometimes laminated matrix mixed with drop material. Random fabric, occasional randomly deformed sandbodies/lenses. Glacio-marine: as above but with marine fauna, foraminifers, shells etc.

Table 1 Schematic genetic classification of tills. Modified after Dreimanis (1989) Banham (1977), Pedersen (1988) and Benn and Evans (1998). Many combinations are possible between the basal tills, especially deformation and lodgement tills.

Fracture types and characteristics in diamict deposits			
Fracture types	**Typical fracture orientation.**	**Fracture size trace-length.**	**Fracture shape (m scale), Surface character and roughness (cm scale)**
Glaciotectonic fractures			
Glacitectonites	Horizontal brecciated shear zones	0.1-1 m thick zones	Small irregular peds (>1-4 cm in diameter)
Shear-zones/shear-planes	Systematic Horizontal sub-horizontal.	2->20 meters long	Shape: Straight- Random Character: Planar-undulating Roughness: slickenside, rough Often silt/sand filled
Low-angle shear- fractures.	Systematic Oblique, down-ice dip, strike perpendicular to ice-movement direction	1->12 meters	Shape: Listric- sigmoidal. Character: Planar-undulating Roughness: slickenside, rough often thin silt or sand fill.
Conjugating shear-fractures. Acute angle between conjugating sets ~30^0	Systematic Oblique to vertical perpendicular to ice-movement direction	1->12 meters	Shape: Straight, listric, sigmoidal Character: Planar-undulating Roughness: slickenside, smooth, rough
Extension fractures	Systematic Sub-vertical, parallel to ice-movement direction.	0.1->10 m	Shape: Random-straight Character: Irregular-undulating Roughness: Rough
Hydro fractures. Downward infilled Upward infilled Clastic dykes.	1-2: Systematic Horizontal to vertical, perpendicular to ice-movement direction, dipping down-ice	0.1->2 m long. Several cm thick	Shape: Random Character: Irregular Undulating. Massive or laminated filling of clay/silt/sand gravel.
Contraction Fractures			
Desiccation fractures. Orthogonal, oriented Orthogonal, random Polygonal non-sorted	Systematic Non-systematic Non-systematic Sub-vertical	Polygons 5-40 cm wide	Shape: Straight-random Character: Irregular columns Roughness: rough. Sediment filled near surface. Primarily in clayey sediments
Ice wedges. Orthogonal, oriented Orthogonal, random Polygonal non-sorted	Systematic Non-systematic Non-systematic Sub-vertical	Polygons 1- >10 m wide	Open, sediment filled fractures, often wedge-shaped irregular fractures. Primarily in sandy sediments
Tensile fracturing due to frost heave.	Non-systematic Sub-vertical	< 1 m deep fractures	Random, irregular fractures, wedge shaped fractures.
Frost cracks. Due to segregation ice.	Non-systematic Micro fractures in sub-horizontal zones	0.3-5 cm spacing. Increasing downwards	Character: Random Shape: irregular. “Brick pattern" Roughness: rough
Neo-tectonic fractures			
Neo-tectonic fractures.	Systematic Vertical/sub-vertical	<10->100m	Character: Straight Shape: planar Roughness: Smooth, slickenside

Table 2 Characteristics of the different fracture types measured in diamict sediments. The Ice-wedges occurs primarily in sandy sediments and has not been investigated during the project, but they are widely distributed in sandy tills and in melt-water sediments in western Jutland, Denmark, and should therefor be included in the diagram.

Table 3: List of soil samples received by IFP and analyse type done on the samples

Numéro	n° Devis IFP ou Nom	n° Bulletin d'analyse ou	Client	Description	Conditionnement	Remarques	Nature polluant	Date	Opérateur(s)	Stockage		
										ambre fro	Réfrigérateur	Autre
Campagne OCtobre 2004												
T-04-054	Stresoil	F0283001	Stresoil	u2 0.2m	flacon verre de 40ml	extraction **methanol**	kérosène	07/10/2004	SP		CLE204/T	
T-04-055	Stresoil	F0283001	Stresoil	u2 0.2m	flacon verre de 40ml	extraction **methanol**	kérosène	07/10/2004	SP		CLE204/T	
T-04-056	Stresoil	F0283001	Stresoil	u2 0.2m	flacon verre de 40ml	extraction **methanol**	kérosène	07/10/2004	SP		CLE204/T	
T-04-057	Stresoil	F0283001	Stresoil	u2 0.2m	flacon verre de 40ml	extraction **methanol**	kérosène	07/10/2004	SP		CLE204/T	
T-04-058	Stresoil	F0283001	Stresoil	u2 0.6m Matrice	flacon verre de 40ml	extraction **methanol**	kérosène	07/10/2004	SP		CLE204/T	
T-04-059	Stresoil	F0283001	Stresoil	u2 0.6m Fracture	flacon verre de 40ml	extraction **methanol**	kérosène	07/10/2004	SP		CLE204/T	
T-04-060	Stresoil	F0283001	Stresoil	u2 0.6m Matrice	flacon verre de 40ml	extraction **methanol**	kérosène	07/10/2004	SP		CLE204/T	
T-04-061	Stresoil	F0283001	Stresoil	u2 0.6m Matrice	flacon verre de 40ml	extraction **methanol**	kérosène	07/10/2004	SP		CLE204/T	
T-04-062	Stresoil	F0283001	Stresoil	u2 0.6m Matrice	flacon verre de 40ml	extraction **methanol**	kérosène	07/10/2004	SP		CLE204/T	
T-04-063	Stresoil	F0283001	Stresoil	u2 0.6m Matrice	flacon verre de 40ml	extraction **methanol**	kérosène	07/10/2004	SP		CLE204/T	
T-04-064	Stresoil	F0283001	Stresoil	u2 0.6m Matrice	flacon verre de 40ml	extraction **methanol**	kérosène	07/10/2004	SP		CLE204/T	
T-04-065	Stresoil	F0283001	Stresoil	u2 0.6m Fracture	flacon verre de 40ml	extraction **methanol**	kérosène	07/10/2004	SP		CLE204/T	
T-04-066	Stresoil	F0283001	Stresoil	u2 0.8m Fracture	flacon verre de 40ml	extraction **methanol**	kérosène	07/10/2004	SP		CLE204/T	
T-04-067	Stresoil	F0283001	Stresoil	u2 0.8m Fracture	flacon verre de 40ml	extraction **methanol**	kérosène	07/10/2004	SP		CLE204/T	
T-04-068	Stresoil	F0283001	Stresoil	u2 0.8m Matrice	flacon verre de 40ml	extraction **methanol**	kérosène	07/10/2004	SP		CLE204/T	
T-04-069	Stresoil	F0283001	Stresoil	u2 0.8m Matrice	flacon verre de 40ml	extraction **methanol**	kérosène	07/10/2004	SP		CLE204/T	
T-04-070	Stresoil	F0283001	Stresoil	u3 1.10m	flacon verre de 40ml	extraction **methanol**	kérosène	07/10/2004	SP		CLE204/T	
T-04-071	Stresoil	F0283001	Stresoil	u3 1.25m	flacon verre de 40ml	extraction **methanol**	kérosène	07/10/2004	SP		CLE204/T	
T-04-072	Stresoil	F0283001	Stresoil	u3 1.75m	flacon verre de 40ml	extraction **methanol**	kérosène	07/10/2004	SP		CLE204/T	
T-04-073	Stresoil	F0283001	Stresoil	u3 2m	flacon verre de 40ml	extraction **methanol**	kérosène	07/10/2004	SP		CLE204/T	
T-04-074	Stresoil	F0283001	Stresoil	u3 2.30m	flacon verre de 40ml	extraction **methanol**	kérosène	07/10/2004	SP		CLE204/T	
T-04-075	Stresoil	F0283001	Stresoil	u4 2.50m Fracture	flacon verre de 40ml	extraction **methanol**	kérosène	07/10/2004	SP		CLE204/T	
T-04-076	Stresoil	F0283001	Stresoil	u4 2.50m Matrice	flacon verre de 40ml	extraction **methanol**	kérosène	07/10/2004	SP		CLE204/T	
T-04-077	Stresoil	F0283001	Stresoil	u4 3.50m Matrice	flacon verre de 40ml	extraction **methanol**	kérosène	07/10/2004	SP		CLE204/T	
T-04-078	Stresoil	F0283001	Stresoil	u4 4.30m Fracture	flacon verre de 40ml	extraction **methanol**	kérosène	07/10/2004	SP		CLE204/T	
T-04-079	Stresoil	F0283001	Stresoil	u4 4.30m Matrice	flacon verre de 40ml	extraction **methanol**	kérosène	07/10/2004	SP		CLE204/T	
T-04-080	Stresoil	F0283001	Stresoil	u2 0.2m	flacon verre de 40ml	extraction **DCM**	kérosène	07/10/2004	SP		CLE204/T	
T-04-081	Stresoil	F0283001	Stresoil	u2 0.2m	flacon verre de 40ml	extraction **DCM**	kérosène	07/10/2004	SP		CLE204/T	
T-04-082	Stresoil	F0283001	Stresoil	u2 0.2m	flacon verre de 40ml	extraction **DCM**	kérosène	07/10/2004	SP		CLE204/T	
T-04-083	Stresoil	F0283001	Stresoil	u2 0.2m	flacon verre de 40ml	extraction **DCM**	kérosène	07/10/2004	SP		CLE204/T	
T-04-084	Stresoil	F0283001	Stresoil	u2 0.6m	flacon verre de 40ml	extraction **DCM**	kérosène	07/10/2004	SP		CLE204/T	
T-04-085	Stresoil	F0283001	Stresoil	u2 0.6m Fracture	flacon verre de 40ml	extraction **DCM**	kérosène	07/10/2004	SP		CLE204/T	
T-04-086	Stresoil	F0283001	Stresoil	u2 0.6m Matrice	flacon verre de 40ml	extraction **DCM**	kérosène	07/10/2004	SP		CLE204/T	
T-04-087	Stresoil	F0283001	Stresoil	u2 0.6m Matrice	flacon verre de 40ml	extraction **DCM**	kérosène	07/10/2004	SP		CLE204/T	
T-04-088	Stresoil	F0283001	Stresoil	u2 0.6m Matrice	flacon verre de 40ml	extraction **DCM**	kérosène	07/10/2004	SP		CLE204/T	

T-04-089	Stresoil	F0283001	Stresoil	u2 0.6m Matrice	flacon verre de 40ml	extraction **DCM**	kérosène	07/10/2004	SP		CLE204/T	
T-04-090	Stresoil	F0283001	Stresoil	u2 0.6m	flacon verre de 40ml	extraction **DCM**	kérosène	07/10/2004	SP		CLE204/T	
T-04-091	Stresoil	F0283001	Stresoil	u2 0.6m	flacon verre de 40ml	extraction **DCM**	kérosène	07/10/2004	SP		CLE204/T	
T-04-092	Stresoil	F0283001	Stresoil	u2 0.8m Fracture	flacon verre de 40ml	extraction **DCM**	kérosène	07/10/2004	SP		CLE204/T	
T-04-093	Stresoil	F0283001	Stresoil	u2 0.8m Fracture	flacon verre de 40ml	extraction **DCM**	kérosène	07/10/2004	SP		CLE204/T	
T-04-094	Stresoil	F0283001	Stresoil	u2 0.8m Matrice	flacon verre de 40ml	extraction **DCM**	kérosène	07/10/2004	SP		CLE204/T	
T-04-095	Stresoil	F0283001	Stresoil	u2 0.8m Matrice	flacon verre de 40ml	extraction **DCM**	kérosène	07/10/2004	SP		CLE204/T	
T-04-096	Stresoil	F0283001	Stresoil	u3 1.10m	flacon verre de 40ml	extraction **DCM**	kérosène	07/10/2004	SP		CLE204/T	
T-04-097	Stresoil	F0283001	Stresoil	u3 1.25m	flacon verre de 40ml	extraction **DCM**	kérosène	07/10/2004	SP		CLE204/T	
T-04-098	Stresoil	F0283001	Stresoil	u3 1.75m	flacon verre de 40ml	extraction **DCM**	kérosène	07/10/2004	SP		CLE204/T	
T-04-099	Stresoil	F0283001	Stresoil	u3 2m	flacon verre de 40ml	extraction **DCM**	kérosène	07/10/2004	SP		CLE204/T	
T-04-100	Stresoil	F0283001	Stresoil	u3 2.30m	flacon verre de 40ml	extraction **DCM**	kérosène	07/10/2004	SP		CLE204/T	
T-04-101	Stresoil	F0283001	Stresoil	u4 2.50m Fracture	flacon verre de 40ml	extraction **DCM**	kérosène	07/10/2004	SP		CLE204/T	
T-04-102	Stresoil	F0283001	Stresoil	u4 2.50m Matrice	flacon verre de 40ml	extraction **DCM**	kérosène	07/10/2004	SP		CLE204/T	
T-04-103	Stresoil	F0283001	Stresoil	u4 3.50m Matrice	flacon verre de 40ml	extraction **DCM**	kérosène	07/10/2004	SP		CLE204/T	
T-04-104	Stresoil	F0283001	Stresoil	u4 4.30m Fracture	flacon verre de 40ml	extraction **DCM**	kérosène	07/10/2004	SP		CLE204/T	
T-04-105	Stresoil	F0283001	Stresoil	u4 4.30m Matrice	flacon verre de 40ml	extraction **DCM**	kérosène	07/10/2004	SP		CLE204/T	
T-04-106	Stresoil	F0283001	Stresoil	u2 E4 bis 0.8 m Fracture	cellule d'emporte piece		kérosène	07/10/2004	SP		CLE204/T	
T-04-107	Stresoil	F0283001	Stresoil	u4 E14 bis2.50 m Fracture	cellule d'emporte piece		kérosène	07/10/2004	SP		CLE204/T	
T-04-108	Stresoil	F0283001	Stresoil	u4 E19 bis 4 m Fracture	cellule d'emporte piece		kérosène	07/10/2004	SP		CLE204/T	
T-04-109	Stresoil	F0283001	Stresoil	E25 0.7m Fracture+Matrice	cellule d'emporte piece		kérosène	07/10/2004	SP		CLE204/T	
T-04-110	Stresoil	F0283001	Stresoil	E25 0.7m Fracture+Matrice	cellule d'emporte piece		kérosène	07/10/2004	SP		CLE204/T	
T-04-111	Stresoil	F0283001	Stresoil	E25 0.7m Fracture+Matrice	cellule d'emporte piece		kérosène	07/10/2004	SP		CLE204/T	
T-04-112	Stresoil	F0283001	Stresoil	E21 4.30 Fracture	flacon verre schott 100ml	solvant HgCl2 à 1 g/l	kérosène	07/10/2004	SP		CLE204/T	
T-04-113	Stresoil	F0283001	Stresoil	E14 2.50 Fracture	flacon verre schott 100ml	solvant HgCl2 à 1 g/l	kérosène	07/10/2004	SP		CLE204/T	
T-04-114	Stresoil	F0283001	Stresoil	E15 2.50m Matrice	flacon verre schott 100ml	solvant HgCl2 à 1 g/l	kérosène	07/10/2004	SP		CLE204/T	
T-04-115	Stresoil	F0283001	Stresoil	E22 4.30 Matrice	flacon verre schott 100ml	solvant HgCl2 à 1 g/l	kérosène	07/10/2004	SP		CLE204/T	
T-04-116	Stresoil	F0283001	Stresoil	E19 bis 4m Fracture u4	flacon verre schott 100ml	solvant HgCl2 à 1 g/l	kérosène	07/10/2004	SP		CLE204/T	
T-04-117	Stresoil	F0283001	Stresoil	E4bis 0.8m Fractureu2	flacon verre schott 100ml	solvant HgCl2 à 1 g/l	kérosène	07/10/2004	SP		CLE204/T	
T-04-118	Stresoil	F0283001	Stresoil	E14bis 2.50 Fracture u4	flacon verre schott 100ml	solvant HgCl2 à 1 g/l	kérosène	07/10/2004	SP		CLE204/T	

T-04-119	Stresoil	F0283001	Stresoil	E2 0.6m Fracture+Matrice	flacon verre schott 100ml	solvant HgCl2 à 1 g/l	kérosène	07/10/2004	SP		CLE204/T	
T-04-120	Stresoil	F0283001	Stresoil	E7 1.5m u3	flacon verre schott 100ml	solvant HgCl2 à 1 g/l	kérosène	07/10/2004	SP		CLE204/T	
T-04-121	Stresoil	F0283001	Stresoil	E11 2.3m u3	flacon verre schott 100ml	solvant HgCl2 à 1 g/l	kérosène	07/10/2004	SP		CLE204/T	
Campagne Novembre 2004												
T-04-131		Stresoil	F0283001	contrat Européen	0511-60-1	flacon verre schott 50ml	envoi par GEUS				09/11/2004	SP
T-04-132		Stresoil	F0283001	contrat Européen	0511-245-1	flacon verre schott 50ml	envoi par GEUS				09/11/2004	SP
T-04-133		Stresoil	F0283001	contrat Européen	0511-320-1	flacon verre schott 50ml	envoi par GEUS				09/11/2004	SP
T-04-134		Stresoil	F0283001	contrat Européen	0511-375-1	flacon verre schott 50ml	envoi par GEUS				09/11/2004	SP
T-04-135		Stresoil	F0283001	contrat Européen	0511-475-1	flacon verre schott 50ml	envoi par GEUS				09/11/2004	SP
T-04-136		Stresoil	F0283001	contrat Européen	0511-535-1	flacon verre schott 50ml	envoi par GEUS				09/11/2004	SP
T-04-137		Stresoil	F0283001	contrat Européen	0511-575-1	flacon verre schott 50ml	envoi par GEUS				09/11/2004	SP
T-04-138		Stresoil	F0283001	contrat Européen	0511-105-2	flacon verre schott 50ml	envoi par GEUS				09/11/2004	SP
T-04-139		Stresoil	F0283001	contrat Européen	0511-220-2	flacon verre schott 50ml	envoi par GEUS				09/11/2004	SP
T-04-140		Stresoil	F0283001	contrat Européen	0511-295-2	flacon verre schott 50ml	envoi par GEUS				09/11/2004	SP
T-04-141		Stresoil	F0283001	contrat Européen	0511-100-3	flacon verre schott 50ml	envoi par GEUS				09/11/2004	SP
T-04-142		Stresoil	F0283001	contrat Européen	0511-180-3	flacon verre schott 50ml	envoi par GEUS				09/11/2004	SP
T-04-143		Stresoil	F0283001	contrat Européen	0511-280-3	flacon verre schott 50ml	envoi par GEUS				09/11/2004	SP
T-04-144		Stresoil	F0283001	contrat Européen	0511-395-3	flacon verre schott 50ml	envoi par GEUS				09/11/2004	SP
T-04-145		Stresoil	F0283001	contrat Européen	0511-480-3	flacon verre schott 50ml	envoi par GEUS				09/11/2004	SP
T-04-146		Stresoil	F0283001	contrat Européen	0511-580-3	flacon verre schott 50ml	envoi par GEUS				09/11/2004	SP

Numéro	n° Devis IFP ou Nom projet	n° Bulletin d'analyse ou n°Etude	Client	Description	Conditionnement	Remarques	Nature polluant	Date	Opérateur(s)	Stockage		
										Chambre froide	Réfrigérateur	Autre
T-05-128			Stresoil	Carotte 1 / U2 0,5m-1m						01/03/2005	YB/SD	
T-05-129			Stresoil	Carotte 2 / U2 1,7m-2,2m						01/03/2005	YB/SD	
T-05-130			Stresoil	Carotte 3 / U3 2,7m - 3,4m						01/03/2005	YB/SD	
T-05-131			Stresoil	Carotte 4 / U4 3,7m-4,4m						01/03/2005	YB/SD	
T-05-132			Stresoil	Carotte 5 / U4 4,9m-5,6m						01/03/2005	YB/SD	